Check for updates

Basin Research

WILEY

Basin Research IAS EAGE

RESEARCH ARTICLE OPEN ACCESS

Latest Cretaceous to Cenozoic Exhumation Patterns in the Northern Andes From the Sedimentary Provenance Record on the Broken Retro-Foreland Putumayo Basin

Giovanny Nova[1] | Mauricio Parra[1] | Agustín Cardona[2] | Brian K. Horton[3] | Victor A. Valencia[4] | Andrés Mora[5] | Cleber Soares[6]

[1]Instituto de Geociências, Universidade de São Paulo, São Paulo, Brazil | [2]Universidad Nacional de Colombia, Sede Medellín, Colombia | [3]Institute for Geophysics and Department of Earth and Planetary Sciences Jackson School of Geosciences, University of Texas at Austin, Austin, Texas, USA | [4]School of the Environment, Washington State University, Pullman, Washington, USA | [5]Ecopetrol, Bogotá, Colombia | [6]Laboratorio ChronusCamp Research—Isotope Geology Laboratory, Itapira, Brazil

Correspondence: Giovanny Nova (gionovar@usp.br)

Received: 8 November 2024 | **Revised:** 22 May 2025 | **Accepted:** 28 May 2025

Funding: This work was supported by National Science Foundation. Agência Nacional do Petróleo, Gás Natural e Biocombustíveis. Fundação de Amparo à Pesquisa do Estado de São Paulo.

Keywords: Amazon Basin | Broken Foreland | Northern Andes | Orogenic Growth | Provenance Analysis

ABSTRACT

The topographic growth of the Eastern Cordillera in the northern Andes of Colombia is a critical event in the tectonic and paleogeographic evolution of the western Amazon Basin. Documentation of early orogenic growth is enabled through multi-proxy provenance signatures recorded in the adjacent retro-foreland basin. In broken foreland basins, basement highs interrupt the lateral continuity of facies belts and potentially mask provenance signals. The Putumayo Basin is a broken foreland basin in western Amazonia at ~1°–3° N, where the Florencia, Macarena, and El Melón-Vaupes basement highs have compartmentalised discrete depocentres during basin development. This study presents new evidence from stratigraphic, conglomerate clast count, sandstone petrography, detrital zircon U–Pb geochronology and novel apatite detrital U–Pb age trace element geochemistry analyses. The results show that the southern Eastern Cordillera (i.e., Garzon Massif) and Putumayo Basin basement highs were initially uplifted during the Late Cretaceous coeval with the Central Cordillera, most likely associated with the collision of the Caribbean Large Igneous Province (CLIP). Distinctive facies distributions and provenance changes characterise the Putumayo Basin over a ~300 km distance from south to north, in the Rumiyaco Formation and Neme Sandstone. Detrital zircon U–Pb ages record a sharp reversal from easterly derived Proterozoic to westerly sourced late Mesozoic–Cenozoic Andean zircons derived principally from the Central Cordillera. Provenance signatures of the synorogenic Eocene Pepino Formation demonstrate the continued exhumation of the Eastern Cordillera as a second-order source area. However, the emergence of the northern intraplate highs modulated the provenance signature due to the rapid unroofing of relatively thinner marine sedimentary cover strata that overlie the Putumayo basement, in comparison to the thicker sequences of the southern basin. The provenance data and facies distributions of the Oligocene–Miocene Orito Group were more heterogeneous due to strike-slip deformation, associated with major plate tectonic reorganisation as the Nazca Plate subducted under the South American margin.

This is an open access article under the terms of the Creative Commons Attribution License, which permits use, distribution and reproduction in any medium, provided the original work is properly cited.

© 2025 The Author(s). *Basin Research* published by International Association of Sedimentologists and European Association of Geoscientists and Engineers and John Wiley & Sons Ltd.

Summary

- Slab flattening of the subducting Caribbean plate produces the early orogenic growth of the Northern Andes.
- Orogenic growth in the southern segment of the Eastern Cordillera began in the Late Cretaceous.
- The uplift of intraplate highs aided the establishment of the Putumayo broken foreland basin.
- Cenozoic provenance data are modulated by the incipient uplift of Colombia's Eastern and Central Cordilleras.
- Northeastern diachronic provenance shift from Cratonic to Andean source in the fragmented Putumayo foredeep.

1 | Introduction

The uplift history of orogenic belts has major implications for the evolution of biodiversity, the organisation of river drainage patterns, climate change and sedimentary discharge (DeCelles et al. 1998, 2011; Mulch 2016; Horton 2018; van Hinsbergen and Boschman 2019; Calvet et al. 2022; Wolf et al. 2021). The uplift of mountains can be recognised through various indirect proxies such as cooling patterns from low-temperature thermochronometry on bedrock samples (e.g., Gallagher 2012), subsidence records in orogenic basins (Bayona et al. 2008, Bayona, Bustamante, et al. 2020; Parra et al. 2009), genomics of biogeographic species (Antonelli et al. 2009; Baker et al. 2014) and stable isotope paleoelevation analysis (Garzione et al. 2017). Multi-method sediment provenance analysis in sandstones is an essential approach in documenting the first stages of mountain uplift (Garzanti and Malusà 2008; Nie et al. 2012). By analysing the compositional changes throughout the stratigraphic record of orogenic basins, their early exhumation histories can be reconstructed and the evolution of orogen systems can be better understood (Spotila 2005; Garzanti et al. 2007; Schildgen and van der Beek 2019).

The Andes are among the largest orogenic belts on Earth and their growth triggered the development of foreland basins adjacent to its eastern flank. Andean mountain building began in the Late Cretaceous (~100 Ma) in the southern Andes (Ramos and Folguera 2005; Folguera et al. 2015), and at ~80–70 Ma in the central and northern Andes (Parra et al. 2012; Spikings et al. 2010; Horton 2018; Bayona 2018; Bayona, Bustamante, et al. 2020). The changes in provenance signatures recorded by foreland basin deposits enable recognition of the early stages of topographic growth, as demonstrated in orogenic systems such as the Pyrenees (Jones et al. 2004; Odlum et al. 2019), Himalayas (DeCelles et al. 1998; Najman et al. 2005), Alps (Garzanti and Malusà 2008) and Andes (Bayona et al. 2008, Bayona, Bustamante, et al. 2020; Nie et al. 2010, 2012; Horton et al. 2016; Horton 2018; Louterbach et al. 2018; Hurtado et al. 2018; Mora et al. 2020; Custódio et al. 2023, 2024). Broken foreland basins represent flexural basins filled with synorogenic sediments and disrupted by basement-involved topographic highs (Horton et al. 2022). Foreland provenance histories commonly evolve with sediment supply originally from catchment areas located at relatively large distances (such as an adjacent craton) followed by sudden shifts to nearby structures in emerging fold-thrust belts (Horton 2018) and/or intraplate uplifts within a broken foreland configuration (Strecker et al. 2011; Saylor et al. 2011; Horton et al. 2022). Such provenance changes leave their imprint on sandstone/conglomerate compositions and detrital zircon U–Pb age distributions (Lawton et al. 1986; Weltje and von Eynatten 2004; Garzanti 2016; Horton 2018).

In the northern Andes, a well-documented cratonward orogenic advance toward the Eastern Cordillera has been modulated by Cenozoic reactivation of inherited structures (Parra et al. 2012; Mora et al. 2006, 2009, 2020) and possibly by Miocene flat slab subduction Siravo et al. (2019) in their northern (Llanos) segment of the retro-foreland basin Bayona et al. (2008). The Cenozoic history of the Llanos Basin is largely derived from the integration of provenance, sedimentologic, subsidence and thermochronometric datasets (Horton et al. 2020 and references therein). Farther south, the orogenic history is poorly documented in the Garzon Massif of the southernmost Eastern Cordillera, which limits the current Putumayo Basin in the retroarc foreland of southern Colombia and northern Ecuador (Figure 1). The Garzon Massif consists of Mesoproterozoic-Tonian (1.4 Ga-0.9 Ga) crystalline rocks and a thin Mesozoic-Cenozoic sedimentary cover section deformed during the Andean Orogeny (van Der Wiel 1991; Anderson et al. 2016; Sandoval et al. 2024).

The current understanding holds that the early Cenozoic subsidence in the northern Andean retro-foreland basins (i.e., Oriente, Putumayo, Upper Magdalena Valley, Eastern Cordillera and Llanos) was associated with basement-involved shortening in the Central Cordillera of Colombia (van Houten and Travis 1968; Montes et al. 2021; Villamizar-Escalante et al. 2021) and Cordillera Real of Ecuador (Higley 2001; Baby et al. 2013; Christophoul et al. 2002; Spikings et al. 2000; Ruiz et al. 2004; Gutiérrez et al. 2019; Vallejo et al. 2021). However, the timing of early deformation in more-eastern segments of the orogen is debated, with a broken foreland segmented by basement uplifts proposed for the Neogene (Montes et al. 2021), Paleogene (Saylor et al. 2011), Maastrichtian (Bayona 2018) and as early as in the Aptian-Albian (León et al. 2023; Calderon-Diaz et al. 2024). The Putumayo sedimentary basin is a broken foreland basin in which the Florencia, Macarena and El Melón-Vaupes basement highs have compartmentalised Cenozoic deposition (Figure 1; Pachón-Parra et al. 2020). These structural highs, which are currently partially buried and have a north–south strike, can be extended into the northern part of the Oriente Basin based on gravimetric and seismic information (Figure 1A; Pachón-Parra et al. 2020; Vargas Gómez 2020). The depocenters that formed adjacent to the basement highs exhibit thicknesses ranging from 4400 to 7000 m. These depocenters are comprised of Cretaceous and Paleogene sedimentary sequences that exhibit a pronounced pinch-out eastwards, particularly against the Florencia and Macarena highs (Pachón-Parra et al. 2020; Vargas Gómez 2020). The timing of basement uplift and the onset of basement exhumation within the Garzon Massif and the attendant evolution of the Putumayo Basin remain poorly understood. The uncertainties relate to limited information on the sediment provenance of Cretaceous-Cenozoic basin fill and their respective source areas. The two main phases of flexural subsidence have been attributed to retroarc shortening and uplift of the Central

13652117, 2025, 3, Downloaded from https://onlinelibrary.wiley.com/doi/10.1111/bre.70041 by Cochrane Colombia, Wiley Online Library on [20/06/2025]. See the Terms and Conditions (https://onlinelibrary.wiley.com/terms-and-conditions) on Wiley Online Library for rules of use; OA articles are governed by the applicable Creative Commons License

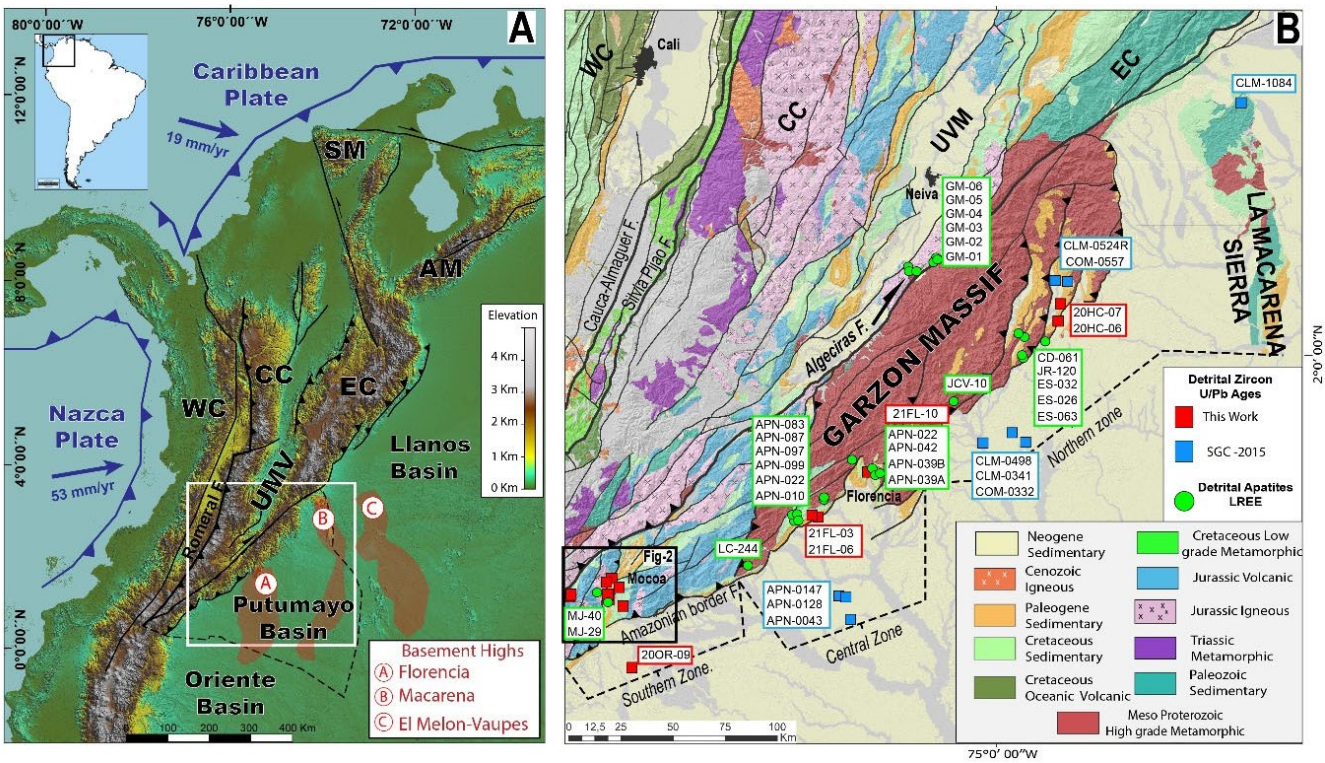

FIGURE 1 | (A) Map of the Northern Andes showing the study area relative to the Western Cordillera (WC), Central Cordillera (CC), Eastern Cordillera (EC), the Oriente, Putumayo and Llanos foreland basins, the intermontane Upper Magdalena Valley Basin (UMV) and the subsurface extension of the basement high uplifts (reddish shading) (Pachón-Parra et al. 2020; Vargas Gómez 2020). (B) Geologic map of the southern part of the Northern Andes with the main faults and exposed rocks, including those from the Garzón Massif. Red squares denote zircon detrital U–Pb ages from this work and blue squares are those from the Colombian Geological Survey (SGC) published by Buchely et al. (2015). Green circles denote samples for apatite U–Pb age-light rare earth element analysis (AUPb-LREE).

Cordillera during the Late Cretaceous-early Palaeocene and Oligocene-Miocene periods (Londoño et al. 2012; Pachón-Parra et al. 2020). These phases led to deposition of clastic depocenters, including an Eocene synorogenic succession related to the initial uplift of the Eastern Cordillera (Londoño et al. 2012; Wolaver et al. 2015; Pachón-Parra et al. 2020).

In this work, we present the first comprehensive documentation of the evolution of the Putumayo Basin and an updated Cenozoic chronostratigraphic framework for the synorogenic clastic succession. We employ a multi-proxy provenance investigation that includes conglomerate clast counts, sandstone petrography, detrital zircon U–Pb geochronology and apatite U–Pb age trace element geochemistry analysis (Tables S1–S5). The provenance changes recorded in the Putumayo Basin are interpreted in terms of exhumational episodes and diachronous orogenic growth of the Northern Andes related to long-term crustal shortening since the Late Cretaceous and oblique collision of the Caribbean oceanic plateau with the northwestern margin of South America (Jaillard et al. 2009; Pindell and Kennan 2009; Bayona et al. 2012; Cardona et al. 2020; Mora et al. 2020).

2 | Geological Setting

The tectonic configuration of the northwestern border of the South American plate has resulted from the collision and accretion of continental and oceanic lithospheric blocks to the Amazonian craton over the last 1400 Ma (Cordani and Teixeira 2007; Cordani et al. 2005). The westernmost Mesoproterozoic rocks of the Amazonian craton comprise the high-grade metamorphic rocks of the Rio Negro-Juruena Province (1800–1500 Ma) and the Rondonia-San Ignacio belt (Cardona et al. 2009; Tassinari and Macambira 1999) or Vaupes belt (1550–1300 Ma) (Sandoval et al. 2024; Moyano-Nieto et al. 2022). Farther west, amphibolite and granulite-grade metamorphic rocks of the adjacent Putumayo Orogen (1100–900 Ma) constitute most of the basement rocks beneath the retroarc Putumayo foreland basin and the Garzon Massif in the Eastern Cordillera of southern Colombia (Ibanez-Mejia et al. 2011; Ibañez-Mejia 2020; Sandoval et al. 2024).

2.1 | Lithology and Ages of the Potential Sources

In Colombia, the Northern Andes are defined by the Western, Central and Eastern cordilleras, which subdivide the adjacent Cauca Valley, Magdalena Valley and Llanos/Putumayo foreland basins (Figure 1). The Western Cordillera consists of Cretaceous low-grade metamorphic belts and oceanic mafic supracrustal rocks. These include oceanic arc and oceanic plateau rocks formed as part of the Caribbean Large Igneous Province (CLIP) (McCourt et al. 1984; Kerr et al. 1996; Jaillard et al. 2009; Pindell and Kennan 2009; Villagómez et al. 2011; León et al. 2018) and Palaeocene-Miocene arc plutons related to the Panama-Choco block (Bayona et al. 2012; Bustamante, Cardona, et al. 2017;

13652117, 2025, 3, Downloaded from https://onlinelibrary.wiley.com/doi/10.1111/bre.70041 by Cochrane Colombia, Wiley Online Library on [20/06/2025]. See the Terms and Conditions (https://onlinelibrary.wiley.com/terms-and-conditions) on Wiley Online Library for rules of use; OA articles are governed by the applicable Creative Commons License

Cardona et al. 2018; Zapata-García and Rodríguez-García 2020). The Panama-Choco block is an intra-oceanic arc that formed in Late Cretaceous time by subduction of the Farallon plate beneath the CLIP and later, in the Oligocene, collided with South America (Montes and Hoyos 2020 and reference therein). The Central Cordillera is split into two domains by the Romeral fault system (Figure 1; i.e., Cauca-Almager, Silvia-Pijao and San Jeronimo faults) (Vinasco and Cordani 2012). The composition of the western domain is similar to that of the Western Cordillera, with Cretaceous arc-related, oceanic metasedimentary and metavolcanic rocks of the Quebradagrande Complex (Jaramillo et al. 2017; Zapata et al. 2019). In contrast, the eastern domain comprises Permian–Triassic migmatites and gneisses, with Late Jurassic Barrovian-type amphibolites derived from an oceanic basalt protolith (Cajamarca Complex) (Maya and González 1995; Blanco-Quintero et al. 2014; Bustamante, Archanjo, et al. 2017). Major units include Permian granitoids such as the La Plata Granite (Rodríguez et al. 2017), a Triassic rift-related sedimentary succession (Payande Group) (Mojica 1980; Cediel et al. 1981) and several Jurassic intrusive bodies emplaced into a continental arc (i.e., Ibague Batholith, Sombrerillo Batholith, Mariquita Stock) (Bustamante et al. 2016; Cochrane, Spikings, Gerdes, et al. 2014; Rodríguez et al. 2018; Zapata et al. 2016; Restrepo et al. 2021) along with coeval volcano-sedimentary intervals such as the Saldaña Formation (Bayona et al. 1994; Bayona, Bustamante, et al. 2020; Mojica and Prinz-Grimm 2000). The Upper Magdalena Valley is a hinterland basin that separates the Central and Eastern cordilleras (Figure 1). Prior to uplift of the Eastern Cordillera, the Upper Magdalena Valley was part of a region with a complex array of extensional basins formed during the Mesozoic, including a thermal-sag basin filled by thick marine Upper Cretaceous strata, overlain by Cenozoic nonmarine deposits associated with a flexural basin (Anderson 1972; van Houten and Travis 1968; Caicedo and Roncancio 1994; Roncancio and Martínez 2011; Gómez et al. 2005).

The aforementioned units are grouped into geochronological provinces according to their crystallisation ages. Whereas the Amazon craton exhibits 1.3–2.0 Ga ages, the Putumayo basement consists of units from the Vaupes belt and Putumayo Orogen with 900–1600 Ma ages (Moyano-Nieto et al. 2022). The pre-Cretaceous crystalline basement includes Palaeozoic sedimentary units with ages of 550–300 Ma, Permian-Middle Triassic granitoids of 300–250 Ma exclusively from the Central Cordillera and Jurassic Andean arc rocks of 220–140 Ma in the southernmost Eastern Cordillera and entire Central Cordillera (Zapata et al. 2016; Rodríguez et al. 2018; Leal-Mejía et al. 2019). The Cretaceous arc has ages ranging from 145 to 65 Ma including granitoids such as Antioquia (99–83 Ma), Mistrato Stock (85 Ma), the Buga (91 Ma) and Jejenes (84 Ma) batholiths in the Central and Western cordilleras (Villagómez et al. 2011; Cardona et al. 2020; Leal-Mejía et al. 2019) and the Condúe-Pinampiro Batholith (94-73 Ma) in the Cordillera Real of northern Ecuador (Spikings et al. 2000; Gutiérrez et al. 2019). In addition, a set of bentonite layers has been identified interstratified in the marine sequences of the Upper Magdalena Valley and Middle Magdalena Valley basins with crystallisation ages spanning a range between 95 Ma and 75 Ma (Villamil and Arango 1998; De la Parra et al. 2024).

A Palaeocene to early Eocene Andean volcanic arc (66 to 50 Ma) was established along the Central Cordillera and northern Caribbean margin of Colombia (Bayona et al. 2012; Bustamante, Cardona, et al. 2017; Barbosa-Espitia et al. 2019; Jaramillo et al. 2022), along with a Late Eocene to Oligocene (40–30 Ma) volcanic arc within the Panama-Chocó block currently exposed in the western flank of the Western Cordillera (Montes et al. 2012; Cardona et al. 2018). Late Oligocene to Neogene ages overlap with the fragmentation of the Nazca Plate into smaller microplates, allowing the establishment of the modern magmatic arc of the Central Cordillera and the emplacement of small plutons in the Central and Western cordilleras (Leal-Mejía et al. 2019; Echeverri et al. 2015; González et al. 2023).

Farther east, the Eastern Cordillera was part of a Mesozoic back-arc basin that was inverted along basement-involved faults during Andean orogenesis (Cooper et al. 1995; Mora et al. 2013). The Eastern Cordillera is flanked by fold-thrust belts with opposite vergences and mixed thin- and thick-skinned geometries in its northern segment (4° N) (e.g., Mora et al. 2020 and references therein). There, the flanking structures involve a marine Cretaceous succession similar to that preserved in the intermontane Upper Magdalena Valley Basin (Horton et al. 2020 and references therein). In contrast, in the southern segment (1°–3° N), the Eastern Cordillera includes basement structures with thick-skinned geometries (Saeid et al. 2017; Wolaver et al. 2015; Mora et al. 2020). Amphibolite-grade and granulite-grade metamorphic basement rocks attributed to the Putumayo Orogen (1100–900 Ma) crop out in the southern Eastern Cordillera near the Florencia area (Figure 1) (Ibanez-Mejia et al. 2011; Priem et al. 1989). The Precambrian subsurface basement of the Putumayo retroarc foreland basin has been characterised using petrology and U–Pb geochronology (Ibanez-Mejia et al. 2011, 2015, 2018) from core samples retrieved beneath the 4–5.5 km-thick Meso-Cenozoic sedimentary cover (Londoño et al. 2012; Pachón-Parra et al. 2020; Beltrán et al. 2022). Other units involved in deformation accommodated by the thick-skinned structures include Early to Middle Jurassic (180–140 Ma) quartz monzonites, granites and limited quartz-diorites attributed to the Mocoa-Sombrerillos batholiths and the coeval volcanoclastic Saldaña Formation (Rodríguez et al. 2018; Bayona, Bustamante, et al. 2020; Sandoval et al. 2024) (Figure 2).

2.2 | Stratigraphy of the Putumayo and Oriente Basins

Cretaceous sediment accumulation in the Putumayo Basin of Colombia commenced in the Aptian (121–113 Ma) with deposition of fluvial-deltaic strata that make up the Caballos Formation (Cáceres and Teatin 1985; Govea and Aguilera 1980; Mora et al. 1998; Núñez 2003) and the equivalent Hollin Formation of the Oriente Basin in Ecuador Vallejo et al. (2021). These basal deposits, which overlie the Proterozoic Garzon Group in the north and Jurassic volcanoclastic rocks of the Saldaña/Misahualli formations in the south (Figure 3), consist of 50–90 m of quartz-arenites and conglomerates and minor variegated mudstones (Montenegro and Barragán 2011; León et al. 2023). The overlying 50 m (northern area) to 600 m (southern area) thick Villeta Formation consists of interbeds of black mudstones, limestones and thin beds of glauconitic quartzarenites of Albian-Santonian age Mora et al. (1998). The Villeta Formation has been correlated with the Napo Formation in the Oriente Basin Vallejo

13652117, 2025, 3, Downloaded from https://onlinelibrary.wiley.com/doi/10.1111/bre.70041 by Cochrane Colombia, Wiley Online Library on [20/06/2025]. See the Terms and Conditions (https://onlinelibrary.wiley.com/terms-and-conditions) on Wiley Online Library for rules of use; OA articles are governed by the applicable Creative Commons License

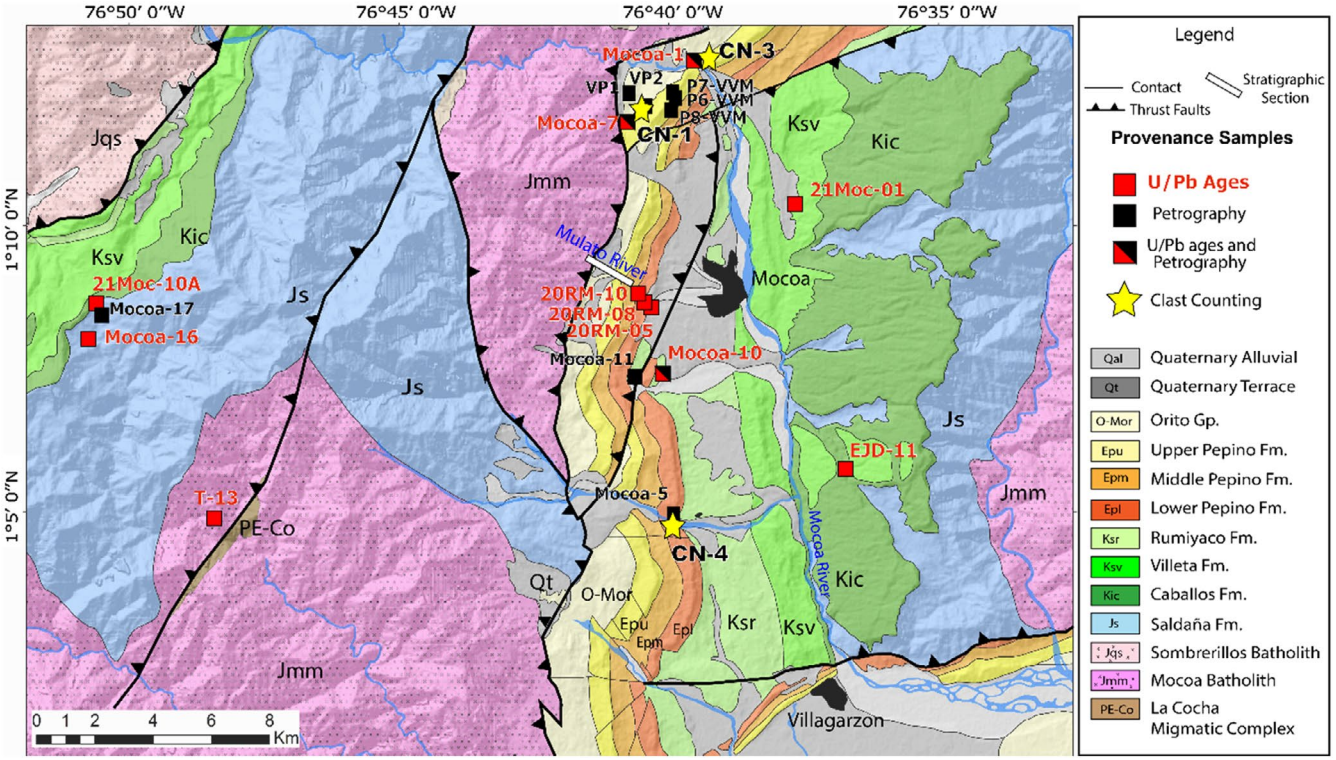

FIGURE 2 | Detailed geologic map of the southern Putumayo Basin (after Núñez 2003). Squares show the locations of new samples for provenance analysis, including zircon U–Pb geochronology (red), sandstone petrographic analysis (black) and conglomerate clast counts (yellow star). The white rectangle shows the location of the stratigraphic section measured along the Mulato River. See location in Figure 1.

et al. (2021) and was deposited in offshore and shoreface environments within an epicontinental sea (Cáceres and Teatin 1985; Govea and Aguilera 1980; Mora et al. 1998). Laterally equivalent facies in the Upper Magdalena Valley Basin farther west include thick marine sequences with two 60–200 m-thick levels of siliceous siltstones that accumulated in the Turonian-Coniacian and Santonian-Campanian (Etayo-Serna 1994; Guerrero et al. 2000; Roncancio and Martínez 2011).

The Cenozoic sedimentary record of the Putumayo Basin consists of a 4.5 km-thick, eastward thinning clastic wedge that is mainly composed of synorogenic conglomerates and sandstones (Londoño 2004). Initial Cenozoic sedimentation was recorded by the 400–1200 m-thick Rumiyaco Formation (Maastrichtian-Palaeocene), which consists of red claystones and siltstones interbedded with sandstone beds (Cáceres and Teatin 1985; Mora et al. 1998; Núñez 2003; Buchely et al. 2015). The correlative Tena Formation in the Oriente Basin has a similar lithology (Figure 3) (Roddaz et al. 2010). In the northern area, near the Florencia and Macarena basement highs, the Garzon Group or, farther south, the Villeta Formation, is unconformably overlain by the Rumiyaco Formation. This unit consists of reddish mudstones that change laterally to medium-grained quartzarenites and locally conglomeratic sandstones of the informally named Neme Sandstone unit (ANH-UPTC 2009; Buchely et al. 2015), representing accumulation in transitional meandering river to deltaic environments (Mora et al. 1998; Vallejo et al. 2017; Bayona 2018).

The 400–500 m-thick Pepino Formation unconformably overlies the Rumiyaco Formation and consists of three members (Cáceres and Teatin 1985; Núñez 2003; Buchely et al. 2015). The lower and upper members contain conglomerates with interlayered sandstones, while the middle member consists of reddish to greyish claystones and siltstones; deposition during the middle Eocene is defined by the palynomorphs *Bombacacidites bellus, Striatriocolpites catatumbus* and *Cicatricosisporites dorogensis* (Mora et al. 1998). The Pepino Formation is correlated with the Tiyuyacu Formation based on the comparable stratigraphic position in the Oriente Basin, includes interbedded tuffaceous beds of early Eocene age (51 ± 5 Ma zircon fission track age; Ruiz et al. 2004) and has been interpreted as deposited in a braided fluvial system with the development of palaeosols (Roddaz et al. 2010; Gutiérrez et al. 2019). The 120–300 m-thick early Oligocene Orteguaza Formation is conformably overlying the Pepino and Tiyuyacu formations and consists of marine, greenish shales and medium to coarse, locally glauconitic sandstones (Figure 3). Fluvial sandstones are dominant in the western sector of the basin (Cáceres and Teatin 1985; Núñez 2003; ANH-UPTC 2009; Roddaz et al. 2010; Christophoul et al. 2002).

The late Oligocene to Pliocene sedimentary records of the Oriente and Putumayo basins show contrasting patterns in terms of grain size and depositional conditions (Figure 3). Whereas the Oriente Basin contains principally fluvial sandstones and conglomerates represented by the Chalcana (late Oligocene-early Miocene), Arajuno (early Miocene) and Chambira (middle-late Miocene) formations (Roddaz et al. 2010; Christophoul et al. 2002), the Orito Group of the Putumayo Basin contains greater proportions of finer-grained deposits, including the Oligocene Orteguaza Formation and overlying Orito-Belen Formation, with early Miocene to Pliocene ages assigned on the

13652117, 2025, 3, Downloaded from https://onlinelibrary.wiley.com/doi/10.1111/bre.70041 by Cochrane Colombia, Wiley Online Library on [20/06/2025]. See the Terms and Conditions (https://onlinelibrary.wiley.com/terms-and-conditions) on Wiley Online Library for rules of use; OA articles are governed by the applicable Creative Commons License

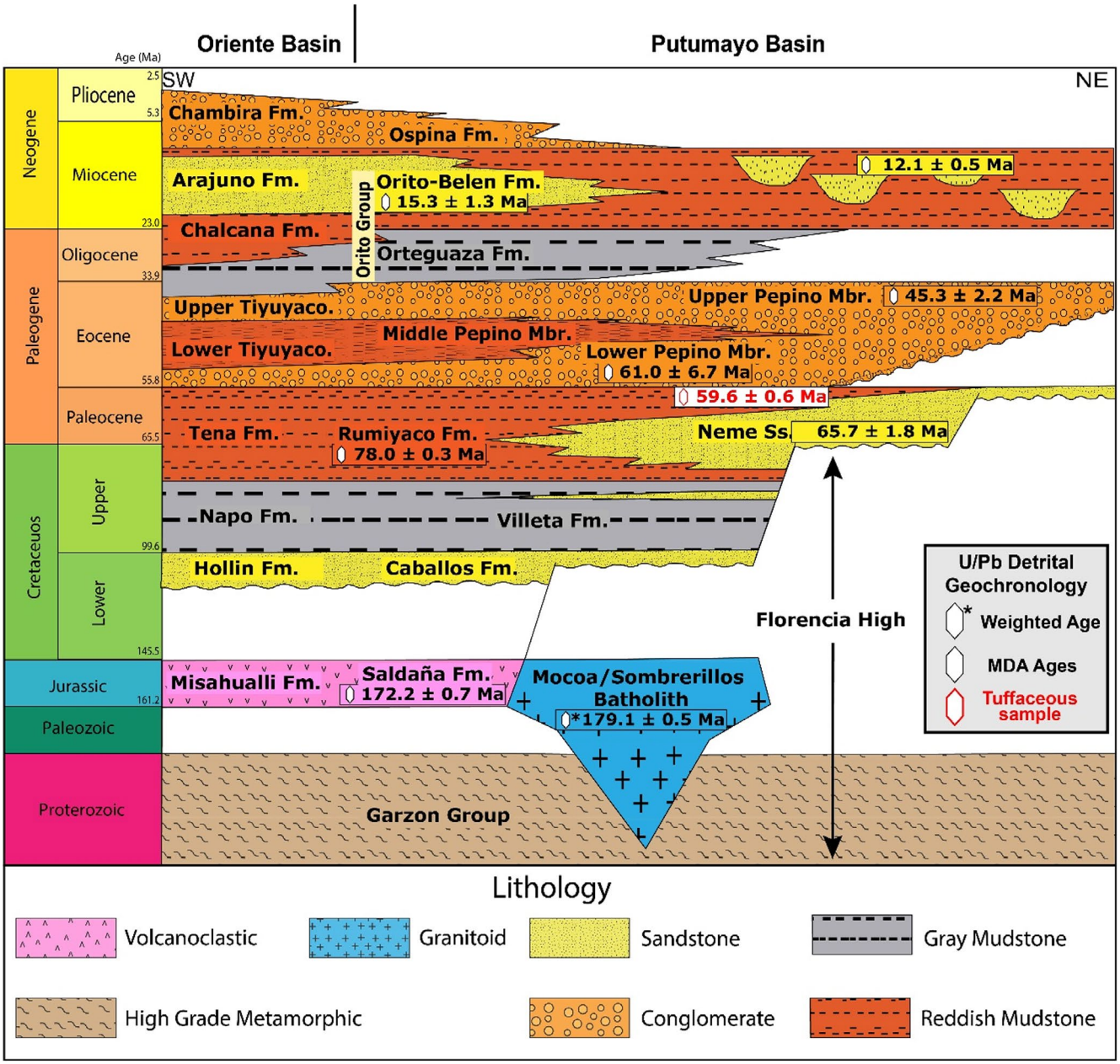

FIGURE 3 | Schematic chronostratigraphic chart of the Putumayo and Oriente basins, showing the distribution of the main lithologic units from the southwestern segments around the Mocoa area to the northeastern segments around the Florencia area. White diamonds show the main maximum depositional ages (MDA) obtained from zircon U–Pb detrital geochronology (Figures 6–8).

basis of palynomorphs such as *Mauritiidites franciscoi* (ANH-UPTC 2009; Buchely et al. 2015). The latter unit consists of heterogeneous mudstones, siltstones, coal beds, and sandy mudstones with calcareous nodules deposited in floodplain swamps and deltas (Cáceres and Teatin 1985; Núñez 2003; Buchely et al. 2015). The overlying Ospina Formation (middle Miocene to Pliocene) consists of sandy mudstones and fine-grained lithic sandstones deposited in mangroves and marshes (Cáceres and Teatin 1985; Núñez 2003; Buchely et al. 2015).

3 | Methods

We report new results on the composition, detrital zircon geochronology, apatite geochronology, and trace element signatures (Table S1) of Cenozoic sedimentary and basement rocks in the Putumayo Basin aimed at characterising the location and configuration of sediment source regions within the northern Andes and Amazonian craton.

3.1 | Stratigraphy and Sedimentology

A 680 m-thick stratigraphic column was measured, sampled and described along the Mulato River section, close to the city of Mocoa (Figure 2). Well-exposed intervals were analysed bed-by-bed using a Jacob staff, while covered intervals were measured with a tape measure and compass. Measured lithologic units include the Rumiyaco Formation, Pepino Formation and Orito Group (Figure 4). Other equivalent intervals of the

13652117, 2025, 3, Downloaded from https://onlinelibrary.wiley.com/doi/10.1111/bre.70041 by Cochrane Colombia, Wiley Online Library on [20/06/2025]. See the Terms and Conditions (https://onlinelibrary.wiley.com/terms-and-conditions) on Wiley Online Library for rules of use; OA articles are governed by the applicable Creative Commons License

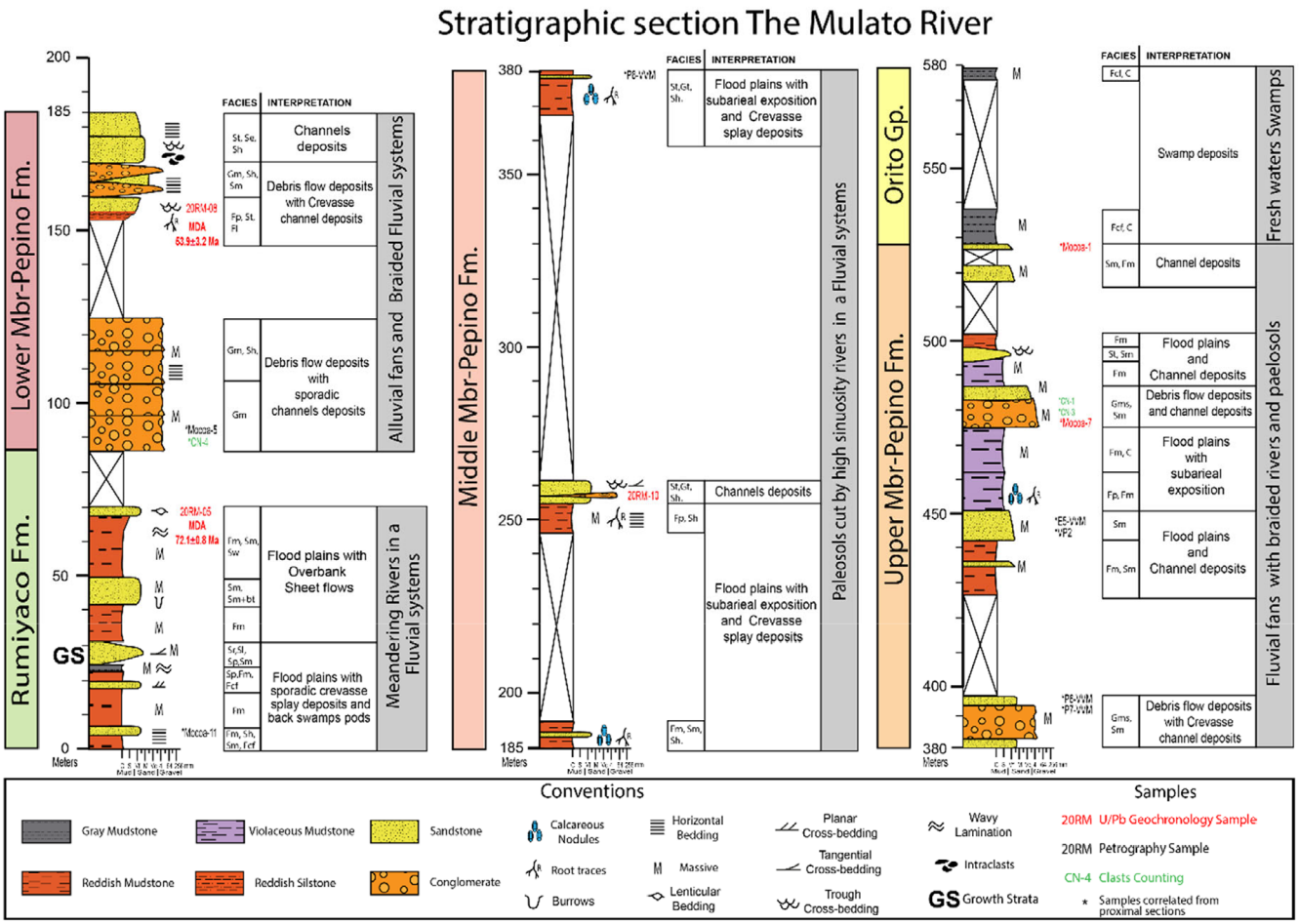

FIGURE 4 | Composite stratigraphic section of Cenozoic deposits of the Putumayo Basin along the Mulato River, including facies associations and interpretations based on Miall (1985, 2006).

Pepino Formation Upper Member and the Orito Group were measured near the Mulato River. Based on the lithology and sedimentary structures, 18 lithofacies and four facies associations (Tables 1 and 2) were recognised within the Rumiyaco, Pepino and Orito–Belen formations following Miall (1985, 2006). A summary of the lithofacies descriptions, facies analysis, the spatial distribution of the facies associations, the associated depositional processes and sedimentary environments is presented in Table 2.

3.2 | Conglomerate Clasts Counting and Sandstone Petrography

Conglomerate clast counts help identify nearby contributors of coarse material within a source-to-sink sedimentary system. Sandstone petrographic analyses further allow for the discrimination of potential source areas over a more extensive region with greater transport distances. Clast counting was performed for thick conglomerate beds within the Lower Member (CN4) and Upper Member of the Pepino Formation (CN1, CN3) and the Orito Group (20OR-06B) (Figure 5; Table S2). The identification of gravel clasts was systematically performed using a rectangular grid with 10 cm spacing until a total of 100 clasts were counted. We also include a clast count reported by Buchely et al. (2015) for the Florencia area.

A total of 11 new thin sections were analysed for sandstone petrography within the Rumiyaco Formation (two samples), the Lower (one sample), Middle (one sample) and Upper (six samples) Members of the Pepino Formation and Orito Group (one sample). Other petrographic analyses (34 thin sections) by Nuñez (Núñez 2003) for the Mocoa area and by Buchely et al. (2015) for the Florencia area from the same lithologic units were compiled for this study (Figure 5; Table S2). Point-count analyses were conducted according to the Gazzi-Dickinson method (Ingersoll et al. 1984) with 400 framework grains counted for each thin section. Thin sections were stained with sodium cobaltinitrite to readily identify potassium feldspar. Samples selected for modal analysis are plotted in QFL ternary diagrams to interpret provenance relations (e.g., Dickinson 1985; Dickinson et al. 1983). Criteria used for distinguishing lithic types (Lawton et al. 1986), matrix types and other components follow those of Dickinson and Suczek (1979). Recalculated petrographic modal data are presented in Table S2.

3.3 | Zircon U–Pb Geochronology

Detrital zircon U–Pb analyses provide absolute age control and identify provenance signatures within Mesozoic–Cenozoic strata of the southern (Table S3.1) and northern (Table S3.2) Putumayo Basin. U–Pb geochronological analyses of individual

13652117, 2025, 3, Downloaded from https://onlinelibrary.wiley.com/doi/10.1111/bre.70041 by Cochrane Colombia, Wiley Online Library on [20/06/2025]. See the Terms and Conditions (https://onlinelibrary.wiley.com/terms-and-conditions) on Wiley Online Library for rules of use; OA articles are governed by the applicable Creative Commons License

TABLE 1 | Architectural elements in fluvial deposits.

Symbol	Lithofacies	Sedimentary environment
Gms	Massive, matrix-supported conglomerate	Subaerial or subaqueous plastic debris flow
Gm	Massive or crudely stratified conglomerate	Lag deposits, longitudinal bars, high hydrodynamic conditions
Gp	Planar stratified conglomerate	Longitudinal bars, deltaic growths from older bar remnants
Gt	Trough cross-bedded conglomerate	Minor channel fills
SGp	Planar cross-bedded gravelly sandstone	Transverse and linguoid gravelly sand bedforms, (2D) dunes and bars
St	Trough cross-bedded, medium to very coarse sandstone	Sinous crest and linguoid (3D) dunes (upper part of the lower flow regime)
Sp	Planar cross-bedded, medium to very coarse sandstone	Transverse and linguoid bars, sand waves, (2D) dunes and bars (medium part of the lower flow regime)
Sh	Horizontally bedded very fine to very coarse sandstone	Plane bed flow (upper flow regime)
Sm	Massive, very fine to very coarse sandstone	Sediment gravity flow deposits
Sr	Ripple cross-laminated, very fine to fine sandstone	Ripples (lower flow regime)
Sl	Low angle (< 10°) cross beds, very fine to very coarse sandstone	Scour fills, washed-out dunes, antidunes
Se	Crude cross-bedding, medium to very coarse sandstone with erosional scours and intraclasts	Scour fills
Fw	Wavy laminated mudstone-siltstones	Overbank deposits with intermittent water level
Fl	Finely laminated mudstone-siltstones	Overbank or waning flood deposits
Fm	Massive mudstone-silstones	Overbank, abandoned channel or drape deposits, backswamp deposits from deposition in suspension with permanent water level
Fcf	Massive greyish to black mudstones	Fresh waters swamps with molluscs
Fp	Massive siltstones-mudstones with rootlets and/or carbonate nodules	Palaeosol
C	Coal, carbonaceous mud, plants fragments, mud films	Swamp deposits

Note: Modified from Miall (1985).

zircon grains from six samples of Jurassic, Cretaceous and Neogene sandstones in the Putumayo Basin were conducted using laser ablation–multicollector inductively coupled plasma–mass spectrometry at the Radiogenic Isotope and Geochronology Laboratory (Washington State University) following the methods and laboratory conditions described by Chang et al. (2006).

In addition, 11 samples were analysed by laser ablation inductively coupled plasma mass spectrometry (LA-ICP MS) at the Arizona LaserChron Center (Gehrels et al. 2006, 2008; Gehrels and Pecha 2014). Zircon grains were ablated with a beam diameter of 20 μm using a Photon Machine Analyte G2 excimer laser equipped with a Helex sample ablation cell. The laser was set at a wavelength of 193 nm, a repetition rate of 8 Hz and a fluence of ~5 J/cm^2. Ablated material was carried in helium to the plasma source of an Element2 HR ICMPS for simultaneous analyses of U-Th-Pb isotopic ratios. For age calibration, measurements were compared to a primary age standard, Sri Lanka zircon (563.5 ± 2.3 Ma; Gehrels et al. 2008) and secondary standards FC-1 ($^{206}Pb/^{238}U$ age of 1099.5 ± 0.5 Ma and $^{206}Pb/^{207}U$ age of 1099 ± 0.6 Ma; Paces and Miller 1993) and R33 ($^{206}Pb/^{238}U$ age of 419.3 ± 0.4 Ma; Black et al. 2004). Uncertainties for $^{206}Pb/^{238}U$ and $^{206}Pb/^{207}Pb$ ages are 1%–2% (1σ error).

For both datasets, reported ages for zircons younger than 1000 Ma represent $^{206}Pb/^{238}U$ ages and $^{206}Pb/^{207}Pb$ ages for zircons older than 1000 Ma, due to the low abundance of ^{207}Pb. This isotope is difficult to measure even for equipment such as LA-ICP-MS, producing discordant ages in very young zircons (< 400 Ma) (Gehrels 2014). Individual analyses with > 20% discordance, > 5% reverse discordance, or 10% internal uncertainty were filtered and removed from further consideration. The data were plotted in age frequency probability plots using the R Isoplot package described by Vermeesch (2018). U–Pb age comparisons with previously published data for various source

13652117, 2025, 3, Downloaded from https://onlinelibrary.wiley.com/doi/10.1111/bre.70041 by Cochrane Colombia, Wiley Online Library on [20/06/2025]. See the Terms and Conditions (https://onlinelibrary.wiley.com/terms-and-conditions) on Wiley Online Library for rules of use; OA articles are governed by the applicable Creative Commons License

TABLE 2 | Facies association in fluvial environments modified from Miall (2006).

Lithofacies association	Lithofacies	Sedimentary environment	
G1	Gm, Sh	Hyperconcentrated and subaerial or subaqueous plastic debris flows	
G2	Gms, Sh	Hyperconcentrated and pseudo plastic debris flows	
S1	Gt, SGp, Sp, Sm, St, Sh, Se	Longitudinal and transverse bars, lag deposits in channels and sand sheets deposited in an upper flow regime	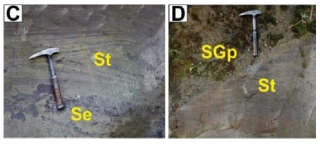
S2	Sm, Sh, Fm	Overbank deposits and sand sheets deposited in crevasse splay	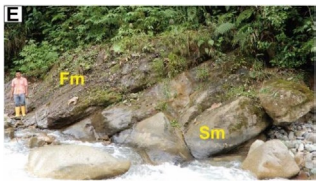
F1	Fp, Fl, Sh, Sm, Sw	Flood plains with overbank deposits and crevasse splay deposits	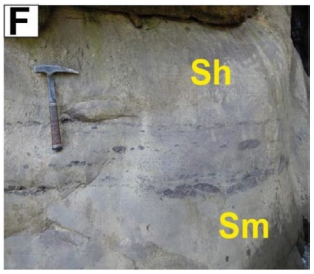
F2	Fp, Fm	Flood plains with subaerial exposition (Palaeosols)	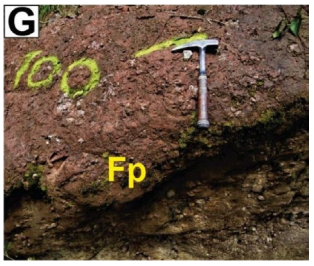

(Continues)

13652117, 2025, 3, Downloaded from https://onlinelibrary.wiley.com/doi/10.1111/bre.70041 by Cochrane Colombia, Wiley Online Library on [20/06/2025]. See the Terms and Conditions (https://onlinelibrary.wiley.com/terms-and-conditions) on Wiley Online Library for rules of use; OA articles are governed by the applicable Creative Commons License

TABLE 2 | (Continued)

Lithofacies association	Lithofacies	Sedimentary environment	
F3	Fcf, C	Back swamp pods or freshwater swamps	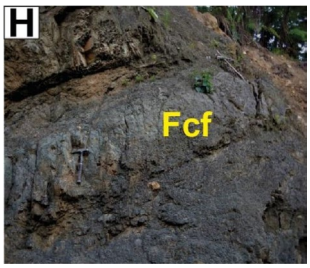

Note: Photographs of the main lithofacies observed along the stratigraphic section of the Mulato River. A 32 cm–long hammer is used for scale. (A) Lithofacies Gm of oligomictic conglomerate dominated by black chert ~75% from the alluvial fans in the Lower Member of the Pepino Formation. (B) Lithofacies Gms of polymictic conglomerate dominated by black chert ~40% and siliceous claystone ~30% from the alluvial fans in the Upper Member of the Pepino Formation. (C) Lithofacies St and Se of cross-bedding sandstones from channel deposits in the Middle Member of the Pepino Formation. (D) Lithofacies SGp and St of sandstone bars from overbank deposits in the Upper Pepino Formation. (E) Lithofacies Sm and Fm of fining-upward sequences from overbank deposits in the Middle Member of the Pepino Formation. (F) Lithofacies Sh and Sm from crevasse splays with muddy intraclasts in the Middle Member of the Pepino Formation. (G) Lithofacies Fp of reddish mudstones from palaeosols in the Middle Member of the Pepino Formation. (H) Lithofacies Fcf of massive greyish mudstones from lacustrine swamps in the Orteguaza Formation.

regions, each with a distinct geochronologic and geodynamic context (Buchely et al. 2015), enabled the characterisation of the relative proportions of grains within different age groups.

3.4 | LA-ICP-MS Apatite U–Pb Geochronology and Multi-Elemental Analysis

The apatite U–Pb ages and trace element analyses (AUPb-LREE) (Table S4) were carried out using the LA-ICP-MS at the ChronusCamp Research Laboratory, applying the method for the direct determination of uranium content using a LA-ICP-MS (Soares et al. 2014). LA-ICP-MS data were normalised using the $^{43}Ca/^{238}U$ ratios of standard (std) and unknown (unk) samples:

$$[U]_{unk} = \left\{\left[\left(^{43}Ca/^{238}U\right)_{unk}\right] / \left[\left(^{43}Ca/^{238}U\right)_{std}\right] \times \left(U_{std}\right)\right\}.$$

The system consists of a UP213nm laser ablation system attached to an Agilent 7800 ICP-MS. A gas mixer (Squid) was connected to the laser ablation system for better homogenisation of the isotope mixture. The analytical work included quantifying fission track ages in apatite (presented in another manuscript) and, therefore, the spot size was chosen to cover the maximum area where spontaneous fission tracks were previously measured using an optical microscope. The laser acquisition routine included (1) warm-up time of 15 s, which is used as a background; (2) 45 s of dwell time, which is the sample ablation time and (3) 30 s for washout delay, which is used to clean the system before analysing the next grain.

The AUPb technique is based on the accumulation of radiogenic ^{206}Pb and ^{207}Pb from radioactive decay of ^{238}U and ^{235}U series in apatites and the ensuing movement of lead (Pb) within the atomic structure of an apatite grain through heat-induced volume diffusion (Paul et al. 2019), which, therefore, offers insights into the thermal history of the apatite grain (Cochrane, Spikings, Chew, et al. 2014). Several studies have determined that the AUPb system closure temperature ranges from 550°C to 450°C, depending on factors such as cooling rates and the size of the apatite crystals (Chew et al. 2012; Cochrane, Spikings, Chew, et al. 2014). Isotopes of ^{204}Pb, ^{206}Pb, ^{207}Pb, ^{208}Pb, 232th and ^{238}U measured through LA-ICP-MS were employed for determining AUPb ages. Madagascar apatite (MAD) crystals (reference age 474.2 ± 0.4 Ma; Thomson et al. 2012) were used as the primary reference material, while McClure apatite grains (523.5 ± 1.5 Ma; Schoene and Bowring 2006) were used for quality control. Data reduction was performed using the "VisualAge_UcomPbine" Data Reduction Scheme (DRS) in the software Iolite, which can account for the presence of variable common Pb in the primary reference material (Paton et al. 2011; Chew et al. 2014). We considered non-dateable grains (as defined by O'Sullivan et al. 2018) as those having uncertainties larger than 20% on the ^{207}Pb-corrected U–Pb age.

Trace element analyses on apatite are diagnostic of their host rock and a faithful recorder of the parent melt geochemistry (O'Sullivan et al. 2020). Trace element data reduction was performed using the X_Trace_Elements_ISDRS in Iolite (Paton et al. 2011), following Chew et al. (2016). Instrumental drift was corrected using NIST 612 as the primary standard, and elemental concentrations were calculated using ^{43}Ca for internal standardisation using stoichiometric abundance of Ca at 39.74 wt% (Chew et al. 2014). In addition, a synthetic apatite crystal (SynAp) was used as a high-chlorine standard. The synthetic apatite crystal (SynAp) served as a high-chlorine standard alongside NIST 612 glass and MAD apatite for determining individual element concentrations.

The apatite trace element provenance consists of discriminating the source of apatites by using the sum of light rare earth elements (LREE) such as ^{139}La, ^{140}Ce, ^{141}Pr and 146 Nd (ΣLREE) normalised to chondrite (Laul 1979). Then, Sr/Y versus the summation of LREE was plotted in a support vector machine apatite classification diagram (SVM plot) that aids in characterising each grain petrogenetically (O'Sullivan et al. 2020). The six broad categories of apatite consist of alkali-rich igneous rocks (ALK); mafic I-type granitoids and mafic igneous rocks (IM); low- and medium-grade

13652117, 2025, 3, Downloaded from https://onlinelibrary.wiley.com/doi/10.1111/bre.70041 by Cochrane Colombia, Wiley Online Library on [20/06/2025]. See the Terms and Conditions (https://onlinelibrary.wiley.com/terms-and-conditions) on Wiley Online Library for rules of use; OA articles are governed by the applicable Creative Commons License

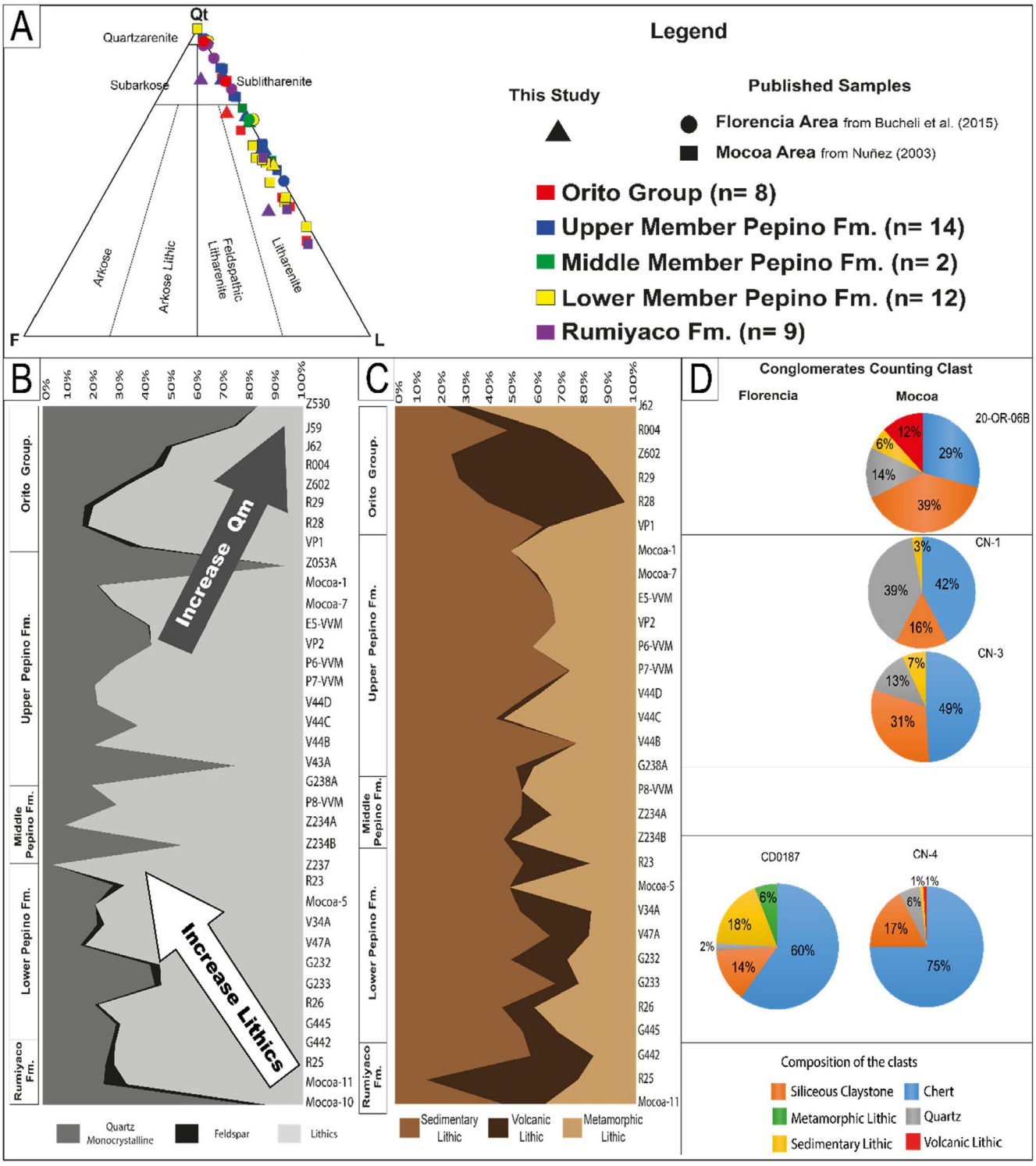

FIGURE 5 | (A) Compositional sandstone petrographic trends (Folk 1980). Ternary diagrams show the dominance of litharenites in the Rumiyaco Formation and the Lower and Middle Members of the Pepino Formation, with sublitharenites and quartzarenites in the Upper Member of the Pepino Formation. (B) Compositional sandstone variations through the stratigraphic record in the Mocoa area showing an upsection decrease in monocrystalline quartz from the Rumiyaco Formation through the Lower Pepino Formation and an increase in monocrystalline quartz within the Orito Group. The opposite trend is shown by the lithic grains. (C) Detailed discrimination of sandstone lithic grains showing an upsection decrease in volcanic lithic material from the top of the Rumiyaco Formation through all members of the Pepino Formation. (D) Compositional results from conglomerate clast counts in the Lower and Upper Members of the Pepino Formation and the Orito Group (Orito-Belen Formation) show an upsection decrease in chert clasts and increases in quartz and volcanic clasts. Photomicrographs of some samples in Figure S2.

13652117, 2025, 3, Downloaded from https://onlinelibrary.wiley.com/doi/10.1111/bre.70041 by Cochrane Colombia, Wiley Online Library on [20/06/2025]. See the Terms and Conditions (https://onlinelibrary.wiley.com/terms-and-conditions) on Wiley Online Library for rules of use; OA articles are governed by the applicable Creative Commons License

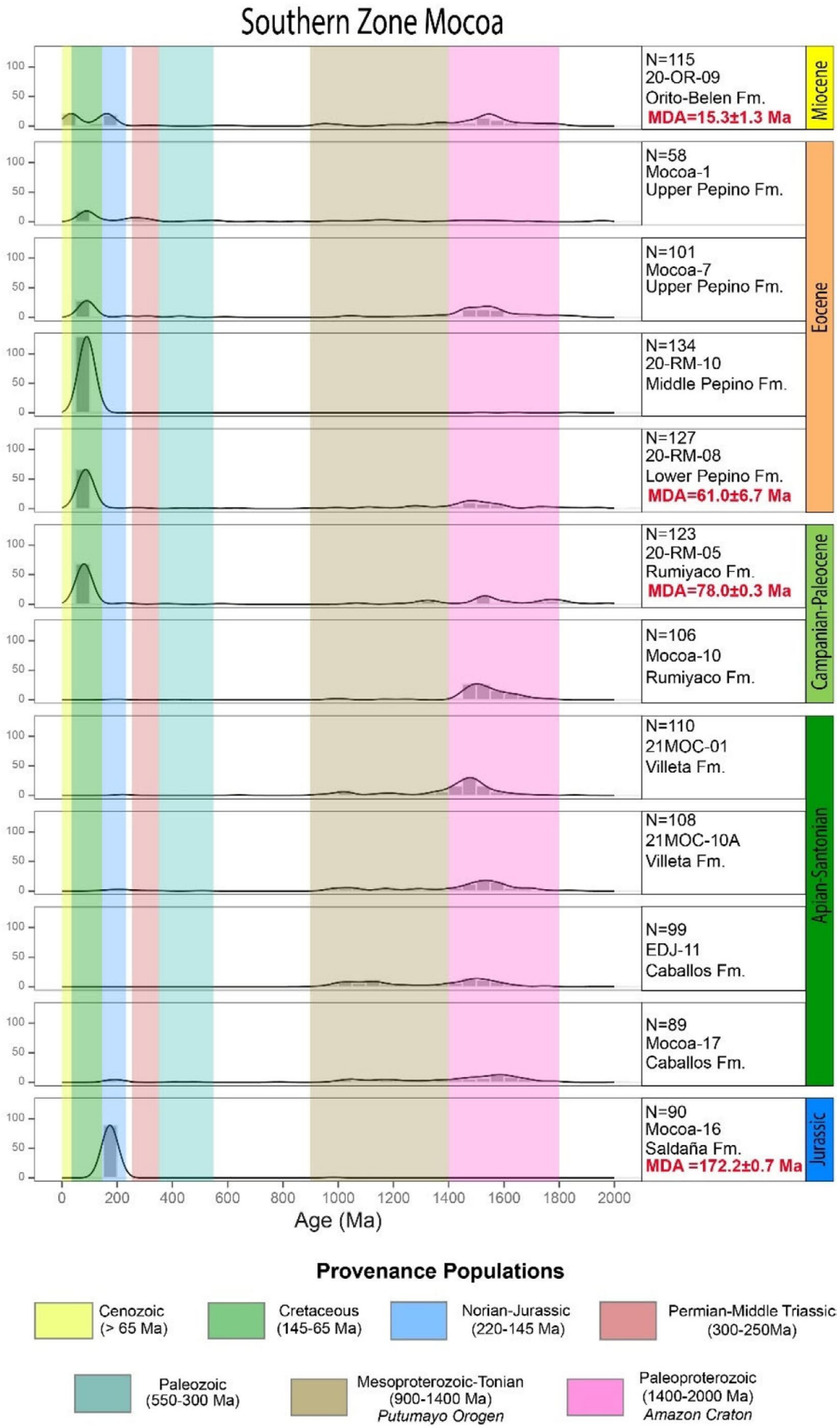

FIGURE 6 | Legend on next page.

13652117, 2025, 3, Downloaded from https://onlinelibrary.wiley.com/doi/10.1111/bre.70041 by Cochrane Colombia, Wiley Online Library on [20/06/2025]. See the Terms and Conditions (https://onlinelibrary.wiley.com/terms-and-conditions) on Wiley Online Library for rules of use; OA articles are governed by the applicable Creative Commons License

FIGURE 6 | Kernel Density Estimate (KDE) plots of detrital zircon U–Pb ages from the Jurassic Saldaña Formation, Upper Cretaceous–Palaeocene Caballos and Rumiyaco formations, Eocene Pepino Formation, and Miocene Orito Group in the southern area (Mocoa) of the Putumayo Basin. The muddy Oligocene succession was not analysed. Note the change in the provenance signal between the Rumiyaco and Pepino formations. MDA ages correspond to the U–Pb age from maximum likelihood age (MLA) (Vermeesch 2021). Because the MLA ages have a better statistical approach that converges to a unique MDA value. See Figure S3 for probability density plots.

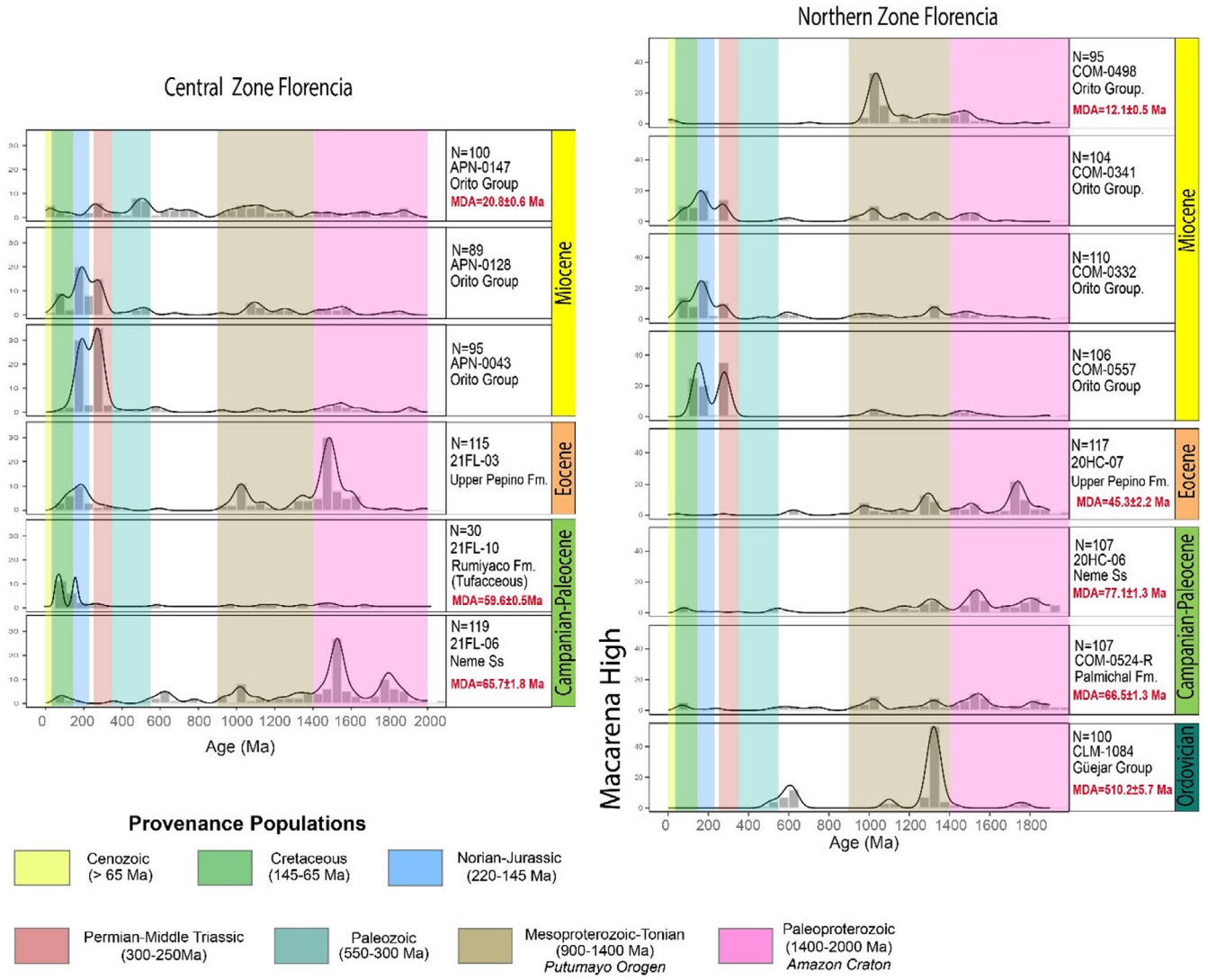

FIGURE 7 | Kernel Density Estimate (KDE) plots of detrital zircon U–Pb ages from the Palaeozoic Güejar Group, Campanian–Palaeocene Neme Sandstone, Palmichal and Rumiyaco formations, Eocene Pepino Formation and Miocene Orito Group. The samples span two regions: a central zone south of the Florencia basement high and a northern zone between the Florencia High and Macarena basement highs. Note the contrasting age of the provenance polarity switch: Eocene in the central zone and Miocene in the northern zone. MDA ages correspond to the U–Pb age from maximum likelihood age (MLA) (Vermeesch 2021). Because the MLA ages have a better statistical approach that converges to a unique MDA value, see Figure S4 for probability density plots.

metamorphic and metasomatic (LM); partial-melts/leucosomes/high-grade metamorphic (HM); S-type and I-type granitoids with high aluminium saturation index (S) and ultramafic rocks including carbonatites, lherzolites and pyroxenites (UM).

4 | Results

The southern segment of the Eastern Cordillera was subdivided into three geographical zones. The southernmost area around the city of Mocoa corresponds to the southern zone, and the northernmost area between the city of Florencia and the La Macarena Range is divided into central and northern zones (Figure 1).

4.1 | Stratigraphy of the Maastrichtian-Cenozoic Putumayo Basin

The three lithologic units described along the Mulato River (Figure 2) are the Rumiyaco and Pepino formations and the base

13652117, 2025, 3, Downloaded from https://onlinelibrary.wiley.com/doi/10.1111/bre.70041 by Cochrane Colombia, Wiley Online Library on [20/06/2025]. See the Terms and Conditions (https://onlinelibrary.wiley.com/terms-and-conditions) on Wiley Online Library for rules of use; OA articles are governed by the applicable Creative Commons License

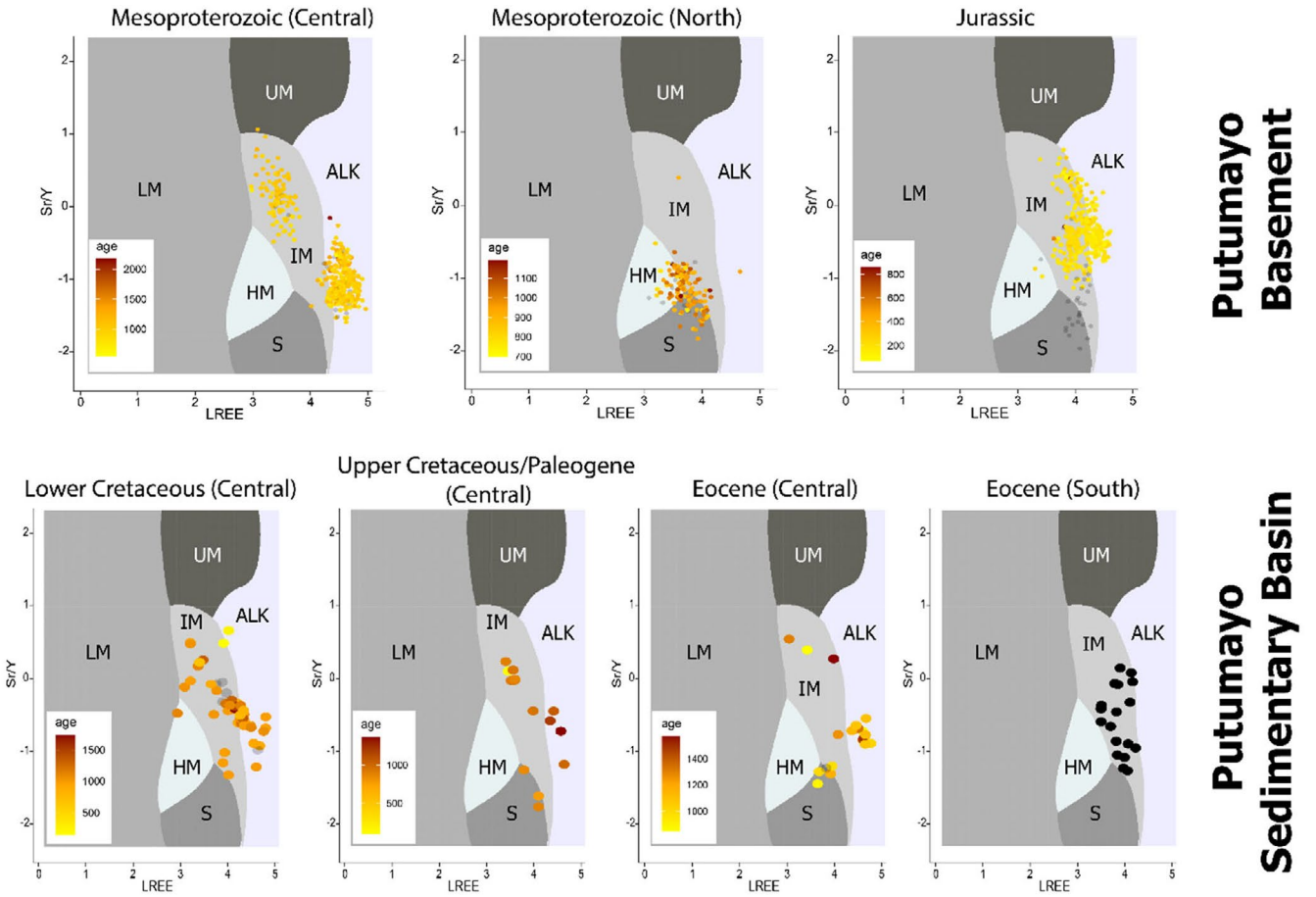

FIGURE 8 | Trace element geochemistry of detrital apatites from Mesoproterozoic basement rocks of the Garzon Group and Jurassic batholiths such as the Algeciras and Mocoa batholiths. Analysed sandstone units include the Lower Cretaceous Caballos Formation, Upper Cretaceous-Palaeocene Rumiyaco Formation and Eocene Pepino Formation. All data are plotted on Sr/Y vs. ΣLREE SVM biplot and coloured by U–Pb age (undated grains in grey or black). Abbreviations for groups: ALK = alkali-rich igneous rocks; IM = mafic I-type granitoids and mafic igneous rocks; LM = low- and medium-grade metamorphic and metasomatic; HM = partial-melts/leucosomes/high-grade metamorphic; S = S-type granitoids and high aluminium saturation index (ASI) 'felsic' I-types; UM = ultramafic rocks including carbonatites, lherzolites and pyroxenites.

of the Orito Group (i.e., Orteguaza Formation). The Rumiyaco Formation has a thickness of 85 m. Upsection, it consists of reddish mudstones interlayered with massive fine grain size sandstones and subordinate grey mudstones grouped into the lithofacies associations F1 and S1 (Figure 4, Table 2). In addition, local very thick and wedge-shaped beds of sandstones corresponding to lithofacies association S2 are related to growth strata with dips varying from 17° to 25°, between 25 m and 50 m of the Mulato River section (Figure S1). According to its lithofacies association, the Rumiyaco Formation can be associated with meandering rivers within a regional-scale fluvial system. The age of deposition for this unit has been indicated as Maastrichtian based on palynomorphs such as *Buttinia andreevi* (Mora et al. 1998).

The Pepino Formation comprises a 195 m-thick intermediate member of mudstone-dominated facies interlayered between the 100 m-thick conglomeratic Lower Member and 150 m-thick sandy Upper Member and is conformably overlying the Rumiyaco Formation. The Lower Member has oligomictic clast-supported boulder conglomerates related to lithofacies association G1 (Figures 4 and S1). Second-order coarsening upward successions of trough cross-bedded sandstones and red mudstones related to lithofacies association S2 and S1 occur interlayered with the conglomerates. According to its lithofacies associations, the Lower Member of the Pepino Formation was deposited in alluvial fans transitioning into a fluvial system of braided rivers.

The Middle Member of the Pepino Formation has a thickness of 195 m and is conformably overlying the Lower Member. Due to the scarcity of outcrops, we were only able to describe three packages (Figure 4). The 5–20 m-thick packages consist of red mudstones with palaeosols and occasionally fining upward successions of massive sandstones with matrix-supported cobble conglomerates related to lithofacies associations F1, F2, S1 and S2 (Table 2). According to its lithofacies association, this member is associated with a high sinuosity channels fluvial system in flood plains. The age of deposition has been identified as middle Eocene based on palynomorphs such as *Bombacacidites bellus, Striatriocolpites catatumbus*, and *Cicatricosisporites dorogensis* (Mora et al. 1998).

The Upper Member of the Pepino Formation has a thickness of 150 m, ~70% of it exposed and conformably overlies the Middle Member (Figure 4). The basal part consists of polymictic matrix-supported granule and pebble conglomerates (Table 2) that

13652117, 2025, 3, Downloaded from https://onlinelibrary.wiley.com/doi/10.1111/bre.70041 by Cochrane Colombia, Wiley Online Library on [20/06/2025]. See the Terms and Conditions (https://onlinelibrary.wiley.com/terms-and-conditions) on Wiley Online Library for rules of use; OA articles are governed by the applicable Creative Commons License

transition upsection to thick-bedded (~10 m) fining upward sequences of cross-bedding sandstones that grade to variegated mudstones and palaeosols. According to lithofacies associations G2, S1, F2 and F1, the Upper Member of the Pepino Formation can be associated with alluvial fans and braided rivers with the coeval development of palaeosols. The age of deposition for this unit has been indicated as late Eocene based on palynomorphs such as *Verrucatosporites cf. usmensis* and *Cicatricosisporites dorogensis* (Mora et al. 1998).

In the study area, we recognised the base of the Orito Group corresponding to the Orteguaza Formation. It consists of 50 m-thick grey mudstones related to lithofacies associations F3 conformably overlying the Upper Member of the Pepino Formation (Figure 4; Table 2) and interpreted as freshwater swamp deposits. The age of deposition for the Orteguaza Formation has been indicated as Oligocene based on palynomorphs such as *Homotryblium floripes, Echiperiporites trianguliformis*, and *Cicatricosisporites dorogensis* from borehole samples (Osorio et al. 2002).

4.2 | Conglomerate Clast Counting

Clast counting was performed in the Upper and Lower members of the Pepino Formation and in one outcrop of the Orito Group close to sample 22OR-09 (Figure 1). Gravel clasts from the Lower Member of the Pepino Formation in the southern section show a high content of chert (75%), followed by siliceous claystones (17%) and quartz (8%). Sparse volcanic (1%) and other sedimentary lithics (1%) clasts are present (Figure 5D). Farther north, in the Florencia area, this unit includes less chert (60%) and quartz (2%) clasts, a similar amount of siliceous claystone clasts (14%) and more lithic fragments, including other sedimentary clasts (18%) and metamorphic clasts (6%) (Buchely et al. 2015). The Upper Member of the Pepino Formation has two slightly contrasting counting results (Figure 5D). The CN-3 sample shows a moderate content of chert clasts (49%), followed by siliceous claystones (31%), quartz (13%) and other sedimentary clasts (7%). While the CN-1 sample has a similar content of chert (42%) and other sedimentary clasts (3%), it contains more quartz (39%) and less siliceous claystone clasts (16%). Upsection, the Orito Group shows a decrease in chert (29%) and quartz (14%) clast contents at the expense of an increase in siliceous claystones (39%) and sedimentary clasts (6%) (Figure 5D). Remarkably, a relatively high content of volcanic clasts (12%) characterises the Orito Group.

4.3 | Sandstone Petrography

Most sandstone samples from this study, as well as those reported by Nuñez (Núñez 2003) in the Mocoa area, have a higher content (> 50%) of lithic grains (L) than the total quartz (Qt) and feldspar (F). In contrast, the sandstones from the Florencia area reported by Buchely et al. (2015) are commonly richer in total quartz (> 50%) than in lithics and feldspar (Figure 5A). The samples from the Rumiyaco Fm. in the Mocoa area are quartzarenites at the base and shift to litharenites and sublitharenites upsection. In contrast, the samples from this unit in the Florencia area are quartzarenites and subtlitharenites of the informal Neme Sandstone unit (Buchely et al. 2015). In the Pepino Formation, sandstones in the Lower Member are litharenites and one sample is a quartzarenite, whereas in the Middle Member they are exclusively litharenite and in the Upper Member, as well as in the Orito Group, sandstones range from litharenite to sublitharenites.

To refine the provenance analysis, samples from the Mocoa area are plotted in stratigraphic order, discriminating between monocrystalline quartz (Qm), feldspar, and total lithics, which include lithic fragments and polycrystalline/chert quartz (Figure 5B). In addition, the abundance of sedimentary, volcanic and metamorphic lithic grains is analysed for the composite stratigraphic section (Figure 5C). Sandstones in the Rumiyaco Formation, as well as the Lower Member of the Pepino Formation, display an upsection decrease in monocrystalline quartz and an increase in lithic grains while containing a low amount of feldspar grains (Figure 5B). Most of the lithics are sedimentary and increase upsection (40%–60%). The volcanic lithic grains (20%–10%) show an upsection decrease, and so do the feldspars (Figure 5C), while the proportion of metamorphic grains (30%–20%) remains stable (Figure 5C). In contrast, sandstones from the Middle and Upper Members of the Pepino Formation show a slight upsection increase in monocrystalline quartz and a decrease in lithic grains. Feldspars disappear in Middle and Upper Pepino members (Figure 5B) and volcanic lithics decrease upsection in the Upper Pepino Formation samples (Figure 5C). The samples from the Orito Group show a minor but persistent proportion of feldspars in all samples, a more accentuated increase in monocrystalline quartz upsection and a decrease in lithic fragments, especially sedimentary grains, from 60% to 20% (Figure 5C). In addition, the metamorphic lithics have an inverse trend, with only a few grains (< 10%) at the base and abundant at the top (~70%). An abrupt increase in volcanic lithics (60%–50%) is seen in the basal samples of the Orito Group.

4.4 | Zircon U–Pb Detrital Geochronology

Detrital zircon U–Pb ages were grouped into seven populations according to potential source areas identified in the northern segment of the Eastern Cordillera and Llanos Basin (Horton et al. 2020), including Cenozoic ages (< 65 Ma), Cretaceous ages (145–65 Ma), Norian-Jurassic ages (220–145 Ma), Permian-Middle Triassic ages (300–250 Ma), Palaeozoic ages (550–300 Ma), Mesoproterozoic-Tonian ages (1400–900 Ma) and Paleoproterozoic ages (1400–2000 Ma). The characteristic provenance signatures were evaluated in several areas: a southern area near Mocoa (Figure 2) and a northern area near Florencia, which is subdivided into a central zone south of the Florencia High and a northern zone between the Florencia High and Macarena-Vaupes High (i.e., Macarena Sierra) (Figure 1).

4.4.1 | Southern Putumayo Basin

In the southern Putumayo Basin, the basal stratigraphic unit, the Jurassic Saldaña Formation, has 99% of its zircon U–Pb ages between 220–145 Ma (Figure 6). In contrast, the Cretaceous Caballos and Villeta formations are dominated by Precambrian ages (~90%) with two populations. First, a Paleoproterozoic population containing ages > 1400 Ma ranges from 53%–57% in the Caballos Formation to 64%–69% in the Villeta Formation.

13652117, 2025, 3, Downloaded from https://onlinelibrary.wiley.com/doi/10.1111/bre.70041 by Cochrane Colombia, Wiley Online Library on [20/06/2025]. See the Terms and Conditions (https://onlinelibrary.wiley.com/terms-and-conditions) on Wiley Online Library for rules of use; OA articles are governed by the applicable Creative Commons License

Second, a Mesoproterozoic-Tonian (1400–900 Ma) population represents 30%–47% of ages in the Caballos Formation and 28% in the Villeta Formation. Although the basal Rumiyaco Formation exhibits a Paleoproterozoic population that forms 90% of the age distribution, the upper Rumiyaco contains reduced amounts of Paleoproterozoic (32%) and Mesoproterozoic-Tonian (10%) ages, and a sharp increase in Cretaceous ages (55%). Upsection, the proportion of Cretaceous ages increases to 51% for the Lower Pepino Formation and 91% for the Middle Pepino Formation. However, this Cretaceous population decreases to 30% in the Upper Pepino Formation, at the expense of the reappearance of both the Paleoproterozoic population, which represents ~20%–50%, and the Mesoproterozoic-Tonian ages, with ~10%–17%. The Upper Pepino Formation (sample Mocoa-1) also shows the first appearance of Permian-Middle Triassic ages, which comprise 17% of the sample's zircon ages. Finally, at the top of the succession, the Orito Group is distinguished by a more heterogeneous population incorporating Paleoproterozoic (46%), Mesoproterozoic-Tonian (9%), Norian-Jurassic (18%) and significant Cenozoic (19%) age groups.

Maximum depositional ages (MDA) were obtained for samples of the Saldaña, Rumiyaco, Lower Pepino and Orito-Belen (Orito Group) formations. Based on the method described by Copeland (2020), which consists of taking the youngest single-grain zircon age for each sample analysed, the calculated MDA values are 155.5 ± 3.8 Ma for the Saldaña Formation, 72.1 ± 0.8 Ma for the Rumiyaco Formation, 53.9 ± 3.2 Ma for the Lower Member-Pepino Formation and 14.0 ± 1.3 Ma for the Orito Group. An alternative method described by Vermeesch (2021) calculates an MDA using all dated zircons and a statistical treatment with a binary mixture of discrete and continuous distributions, which converge on a Maximum Likelihood Age (MLA). Using this method, the MLAs are 177.3 ± 0.3 Ma for the Saldaña Formation, 77.9 ± 0.1 Ma for the Rumiyaco Formation, 62.0 ± 3.5 Ma for the Lower Member-Pepino Formation and 15.7 ± 0.6 Ma for the Orito Group. Furthermore, the weighted average age from the three youngest zircons (Y3Z) is 162.0 ± 3 Ma for the Saldaña Formation, 72.8 ± 1.3 Ma for the Rumiyaco Formation, 70.0 ± 2.1 Ma for the Lower Member-Pepino Formation and 18.6 ± 0.8 Ma for the Orito Group. As suggested by Vermeesch (2021), we chose the MLA ages as the maximum depositional ages because the algorithm is a statistical approach that converges to a unique MDA value and successfully recovers the depositional age for detrital U/Pb ages, producing meaningful results.

4.4.2 | Northern Putumayo Basin

In the northern Putumayo Basin, U–Pb analyses were obtained in the Palaeozoic Güejar Group, which is part of the "basement" of the basin, the Rumiyaco Formation, its laterally equivalent Neme Sandstone and Palmichal Formation in the Macarena Range, the Pepino Formation and the Orito Group. As in the southern area, Precambrian ages are present in all units (Figure 7). The Palaeozoic Güejar Group has a dominant Mesoproterozoic-Tonian age (69%) and minor (7%) Paleoproterozoic ages. In contrast, upsection, the Campanian-Palaeocene Palmichal Formation and Neme Sandstone and Eocene Upper Pepino Formation yield Paleoproterozoic ages ranging from ~50%–60%, with Mesoproterozoic-Tonian ages decreasing to ~30%. The Upper Pepino has a distinctive peak at 1700 Ma ages that exceed that of other units.

In the central zone, a similar pattern is observed for the Neme Sandstone and Upper Pepino Formation. Palaeozoic ages are significant for the Neme Sandstone (9%) in the central zone, but in the northern zone, this population is present in the Palmichal Formation (8%) and Güejar Group (20%), including the youngest Palaeozoic MDA of 498.1 ± 8.4 Ma with a Y3Z age of 509.0 ± 6.1 Ma and MLA of 510.2 ± 5.7 Ma. The first appearance of a moderate Jurassic-Norian population (10%) occurs in the Upper Pepino Formation in the central zone, whereas the Orito Group shows a relative increase in this population with values of ~30% in both the central and northern zones, and a reduction of Precambrian ages to ~10%–30% Mesoproterozoic-Tonian ages and ~ 5%–15% Paleoproterozoic ages. Another shift involves increasing Permian-Middle Triassic ages, with values ranging from 10%–40% in the Orito Group of the central and northern zones. Two exceptions to this pattern in the Orito Group include sample COM-0498 (northern zone) with the reappearance of Precambrian ages with 95% and a higher peak (89%) of 1100 Ma, and sample APB-0147 (central zone) with a more heterogeneous distribution involving chiefly Mesoproterozoic-Tonian (40%) and Paleoproterozoic ages (23%) and moderate Palaeozoic (20%), Permian-Middle Triassic (10%) and Cenozoic (5%) ages.

MDAs were determined from the youngest zircon ages, with 65.7 ± 0.9 Ma for the Neme Sandstone and 64.4 ± 1.3 Ma for the Palmichal Formation, while the Y3Z ages are 73.1 ± 1.2 Ma and 65.5 ± 1.5 Ma and MLAs are 65.7 ± 1.8 Ma and 66.5 ± 1.3 Ma, respectively. Thirty zircons from a tuffaceous palaeosol capping the Neme Sandstone were dated (sample 21FL-10; Figure 3) and provide an MLA of 59.6 ± 0.5 Ma and a Y3Z age of 59.1 ± 1.2 Ma (Figure S4). The Orito Group contains few zircons of Cenozoic age (1%–5%), but MDA values of 19.4 ± 0.7 Ma and 12.0 ± 0.3 Ma are reported for the youngest zircons from samples APN0147 and COM0498, respectively. Furthermore, the Y3Z ages for these same samples are 20.6 ± 0.6 Ma and 12.9 ± 0.4 Ma and MLA ages are 20.8 ± 0.6 Ma and 12.1 ± 0.5 Ma, respectively.

4.5 | Apatite U–Pb Ages and Trace Elements

We obtained trace element geochemical data for apatite grains from the Putumayo basement and basin fill, including 10 samples from the Precambrian metamorphic rocks of the Garzon Group, five samples from Jurassic batholiths (Mocoa and Algeciras granitoids) and seven samples from the sedimentary cover, including two samples from the Caballos Formation, two samples from the Rumiyaco Formation (including the Neme Sandstone) and three samples from the Pepino Formation (Table S4). We separately obtained apatite U–Pb ages for all of these samples, with the exception of two samples from the Mocoa area in the south (Figure 8).

The Sr/Y vs. ΣLREE biplots (Figure 8) allow categorization of apatites from the Putumayo basement into three main sources: (1) Mesoproterozoic-Tonian apatites of the Garzon Group with

13652117, 2025, 3, Downloaded from https://onlinelibrary.wiley.com/doi/10.1111/bre.70041 by Cochrane Colombia, Wiley Online Library on [20/06/2025]. See the Terms and Conditions (https://onlinelibrary.wiley.com/terms-and-conditions) on Wiley Online Library for rules of use; OA articles are governed by the applicable Creative Commons License

U–Pb ages ranging from 900–1500 Ma and discriminating fields of I-type granitoids (IM) and alkali-rich igneous rocks (ALK); (2) Late Mesoproterozoic-Tonian apatites with U–Pb ages ranging from 800–1100 Ma and discriminating fields of partial-melts/leucosomes/high-grade metamorphic (HM), S-type/I-type granitoids with high aluminium saturation index (S) and I-type granitoids (IM); and (3) apatites of the Mocoa and Algeciras batholiths with U–Pb ages ranging from 180–200 Ma and discriminating fields of I-type granitoids (IM), alkali-rich igneous rocks (ALK) and S-type/I-type granitoids with high aluminium saturation index (S).

The apatites from the Lower Cretaceous Caballos Formation plot in the IM and ALK provenance fields with U–Pb ages ranging from 1500–500 Ma but with a high dominance of 1000–1200 Ma ages. The Upper Cretaceous-Paleogene Rumiyaco Formation apatites plot dispersed in the IM, ALK and S fields with U–Pb ages ranging from 1100–500 Ma. Similar to the Rumiyaco Formation apatites, the Eocene Pepino Formation displays dispersed data in the IM, ALK and S fields with U–Pb ages ranging from 1400–1000 Ma. In contrast, the Eocene Pepino Formation in the southern area of Mocoa shows clustered apatites in the IM field.

5 | Discussion

Late Cretaceous–Cenozoic construction of the Andean orogenic belt prompted the development of retroarc foreland basins (Horton 2018). Our results demonstrate that the initial uplift of the northern Andes is recorded by clastic deposits of the Putumayo Basin through changes in the sediment provenance and depositional conditions. These changes commenced in the Late Cretaceous but were not temporally or spatially uniform throughout the foreland region in southern Colombia and northern Ecuador. The following synthesis discusses the implications of the new compositional, geochemical and chronostratigraphic datasets on orogenic growth in the northern Andes, evolution of the Putumayo Basin and the Cenozoic palaeogeography of western Amazonia.

5.1 | Depositional Environments

The Mesozoic-Cenozoic stratigraphic record of the Putumayo Basin shows a change from a Cretaceous rift to a thermal-sag basin with marine conditions represented by the Caballos and Villeta formations to a Cenozoic nonmarine foreland basin with predominantly fluvial sedimentation (Figure 9A; Londoño et al. 2012). Cenozoic sedimentation in the Putumayo Basin started with the Late Cretaceous/Palaeocene deposition of the Rumiyaco Formation. The uppermost Rumiyaco in the Mulato River section is composed of sandstones and red mudstones that accumulated in meandering fluvial systems (Figures 4 and 9B). In contrast, in the Florencia area, reddish mudstones change to coarse-grained quartzarenites of Neme Sandstone that

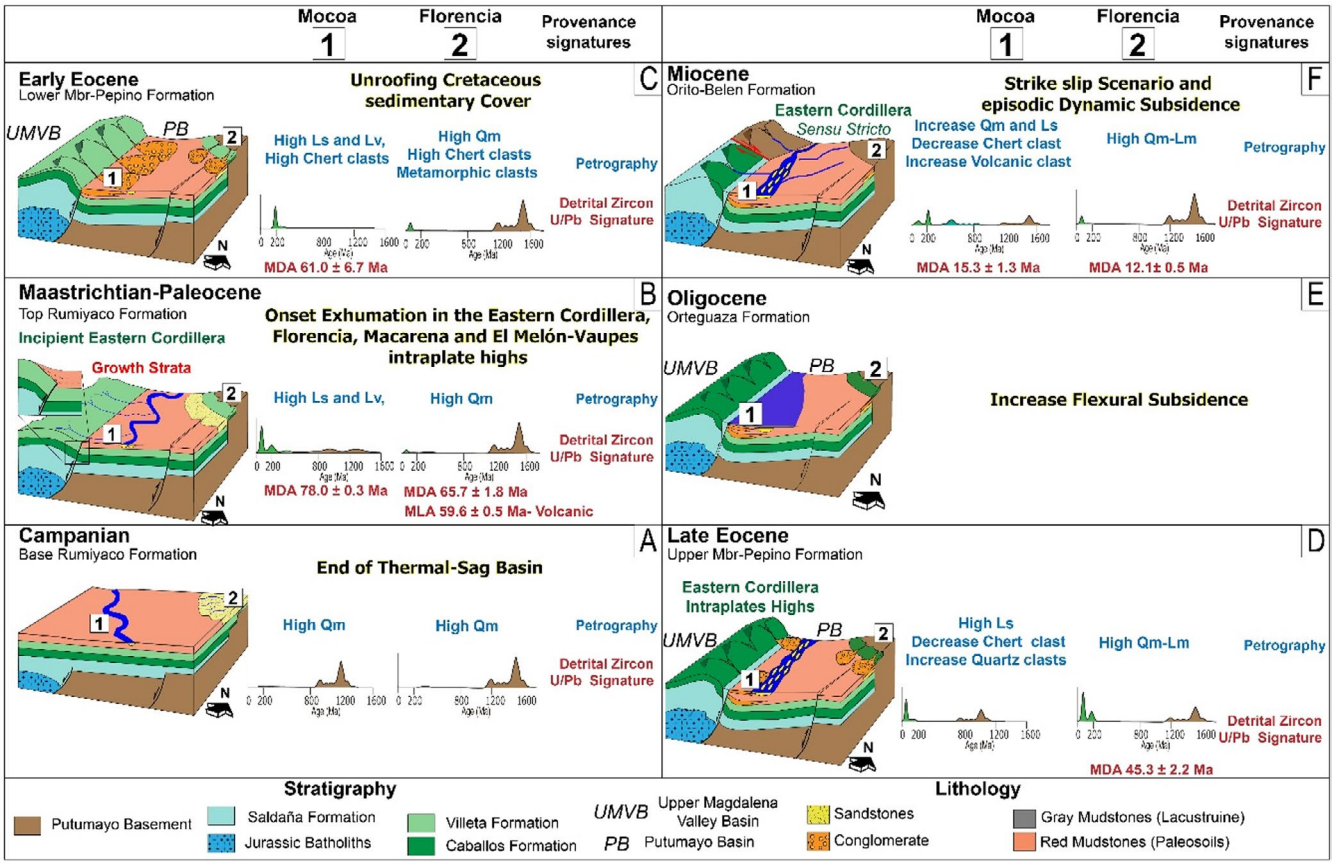

FIGURE 9 | Schematic block diagrams showing the paleoenvironmental evolution of the Putumayo Basin from the southern (1-Mocoa) to the northern (2-Florencia) areas. Six stages are shown (A) Campanian (B) Maastrichtian-Palaeocene (C) Early Eocene (D) Late Eocene (E) Oligocene and (F) Miocene. Schematic changes in detrital zircon U–Pb provenance signatures are represented in each stage, as well as the dominant sandstone composition. Maximum depositional ages (MDA) and Maximum Likelihood Age (MLA) are included.

13652117, 2025, 3, Downloaded from https://onlinelibrary.wiley.com/doi/10.1111/bre.70041 by Cochrane Colombia, Wiley Online Library on [20/06/2025]. See the Terms and Conditions (https://onlinelibrary.wiley.com/terms-and-conditions) on Wiley Online Library for rules of use; OA articles are governed by the applicable Creative Commons License

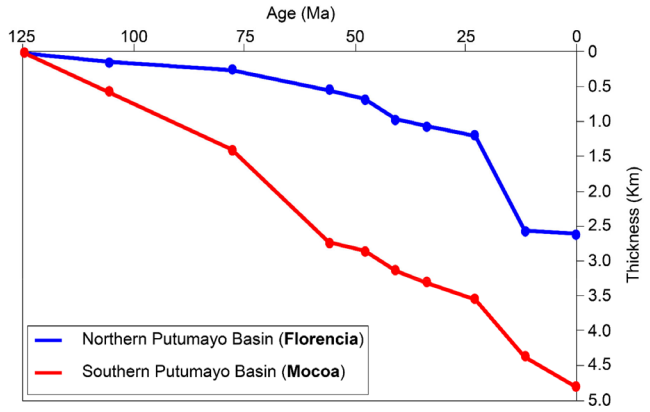

FIGURE 10 | Total subsidence history based on decompacted sediment accumulation for the Putumayo Basin comparing the two areas of the northern segment (Florencia) and the southern segment (Mocoa). Data from SGC-ANH (2022), Caceres and Teatin (Cáceres and Teatin 1985), Londoño (2004), Osorio et al. (2002), and Mora et al. (1998).

were deposited in marine-influenced deltaic systems (Buchely et al. 2015; Bayona 2018). A northward trend toward coarser-grained facies has been interpreted as the main evidence of early uplift of the Eastern Cordillera along the intraplate basement highs (i.e., Florencia, Macarena and El Melón-Vaupes), instead of a fall of eustatic sea level, setting up a broken foreland basin configuration (Bayona 2018; Bayona, Bustamante, et al. 2020; Pachón-Parra et al. 2020). In addition, we identified growth strata in the upper beds of the Rumiyaco Formation (Figures 4 and S1), which have been identified in outcrops (ANH-UPTC 2009; Buchely et al. 2015) to the north in the Florencia area and seismic sections in the south of the Putumayo Basin (Corredor et al. 2019; Beltrán et al. 2022).

The overlying synorogenic Eocene Pepino Formation, whose lower member is characterised by thick beds of oligomictic conglomerates deposited in alluvial fans (Figure 9C), has also been documented from wells drilled in the southern area of the Putumayo Basin near the boundary with Ecuador (Cáceres and Teatin 1985; Govea and Aguilera 1980; Mora et al. 1998). The overlying Middle Member has thick sequences of red mudstones and the development of palaeosols recording a change to a depositional environment with lower energy conditions in a fluvial system with high sinuosity, probably meandering rivers (Figure 4). The resumption of fluvial higher energy conditions dominates the basin during the accumulation of the polymictic conglomerate and sandstones of the Upper Member along braided river systems. Variegated and red mudstones from the Upper Member have been interpreted as palaeosols (Figures 4 and 9D). These second-order patterns of coarsening upward sequences between the Rumiyaco Formation/Lower Pepino Formation in the early Eocene and Middle/Upper Pepino Formation in the late Eocene are not part of the typical sedimentation pattern for synorogenic sediments in the foredeep of a wide and continuous foreland basin (Londoño et al. 2012; Horton et al. 2010). Instead, they are the product of local changes in the subsidence for the Mocoa area, which is higher than the Florencia area, with an increase since the Oligocene in both sectors of the basin (Figures 9E and 10). The low subsidence in the Florencia area results in the partial exposure of basement highs at the surface. This is reflected in the lateral facies changes of the Rumiyaco Formation in the Palaeocene and the persistent provenance of the Putumayo Basement in the Pepino Formation.

For instance, the thickness of the Pepino Formation decreases abruptly northward from ~600 m in the Mocoa area to ~300 m in the Florencia area; the lateral facies change is also accompanied by thickness decrease in the Campanian-Palaeocene Rumiyaco Formation and Neme Sandstone (Figure 3). According to our field observations, this sequence is condensed into a 100 m section over the Florencia High. This suggests that in the Putumayo Basin, a variety of depocenters with distinct accommodation space emerged during the Paleogene, collectively shaping the thickness of these synorogenic sequences. These patterns are analogous to those documented in the northern segment of the Eastern Cordillera with the development of several synorogenic depocenters in the Paleogene (Bayona et al. 2013; Bayona, Baquero, et al. 2020), resulting in the contrasting stratigraphic patterns, subsidence histories and provenance shifts typical of broken foreland basins (Horton et al. 2022 and references therein).

5.2 | Provenance Analysis and Exhumation Episodes

The zircon U–Pb detrital ages from the Jurassic Saldaña Formation display a unimodal 190–160 Ma population with a maximum depositional age (MDA) of 155.5 ± 3.8 Ma. This MDA suggests deposition synchronous with extensive Jurassic arc volcanism and batholith emplacement in the northern Andes, such as the Mocoa and Sombrerillos batholiths (Bustamante et al. 2016; Rodríguez et al. 2018; Zapata et al. 2016; Bayona, Bustamante, et al. 2020; Restrepo et al. 2021). Furthermore, the apatite U–Pb ages ranging from 200–180 Ma for these Jurassic batholiths show a geochemical signature from alkaline/I-type granitoid (Figure 8), compatible with shallow emplacement Chavarría et al. (2022).

The Cretaceous Caballos, Villeta and basal Campanian-Palaeocene Rumiyaco formations have two dominant zircon U–Pb detrital age populations, a > 1600 Ma population from the Amazonian Craton and a 1600–900 Ma population from the Putumayo basement source (Cardona et al. 2009; Cordani and Teixeira 2007) (Figures 6 and 7). The presence of Mesoproterozoic AUPb ages with important alkaline and I-type plutonic contributions suggests the main sources in the central zone of the Putumayo basement (Figure 9) cropping out in the Florencia High as also documented with zircon U–Pb ages (León et al. 2023). The increase in Paleoproterozoic ages from the cratonic source suggests a basin eastward widening associated with thermal-sag until the Campanian (Figure 11A). In addition, the Mocoa-17 sample from the Caballos Formation and both samples from the Villeta Formation have few zircons (< 5%) with Jurassic ages, which indicates that the fluvial-transitional system of the Caballos Formation and the shallow marine system of the Villeta Formation were eroding incipient rift-shoulders uplifted from the Central Cordillera arc system to the west of the basin.

13652117, 2025, 3, Downloaded from https://onlinelibrary.wiley.com/doi/10.1111/bre.70041 by Cochrane Colombia, Wiley Online Library on [20/06/2025]. See the Terms and Conditions (https://onlinelibrary.wiley.com/terms-and-conditions) on Wiley Online Library for rules of use; OA articles are governed by the applicable Creative Commons License

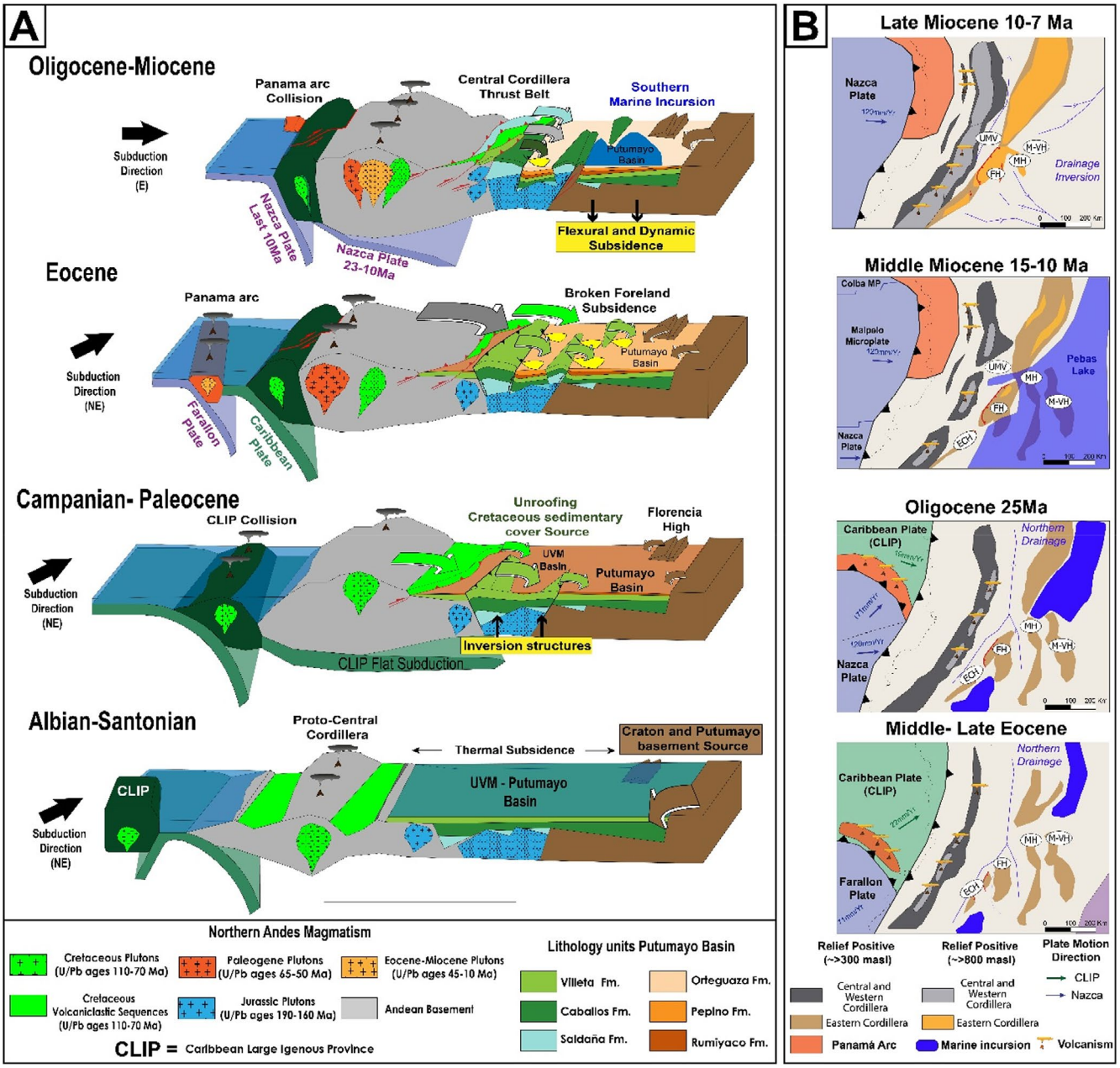

FIGURE 11 | (A) Tectonic model of the Putumayo Basin showing the collisional events that triggered the inversion of preexistent Jurassic rift sequences during the Upper Cretaceous and their influence in the provenance sources from the synorogenic deposits. Brown arrows suggest Amazonian and Putumayo basement sources, dark green arrows suggest a provenance source from unroofing of the Cretaceous sedimentary cover in the Eastern Cordillera. Grey, light blue and green arrows suggest Andean sources from thrust slivers in the Central Cordillera basement, Jurassic arc and Cretaceous volcaniclastic sequences, respectively. (B) Paleogeographic maps of the middle Eocene to Miocene in the Northern Andes showing various events of marine incursions and their respective extents, which are limited by the basement highs including the incipient Eastern Cordillera High (ECH), Florencia High (FH), Macarena High (MH) and El Melon-Vaupes High (MVH). In contrast, the middle Miocene show the marine incursion of the Pebas system established in a significant portion of the Western Amazon Basin.

5.2.1 | Maastrichtian-Palaeocene Provenance

Following the episode of thermal-sag basin formation between Maastrichtian and Palaeocene (Figures 9B and 11A), an abrupt change in detrital zircon U–Pb age populations is observed within the Rumiyaco Formation, in between samples Mocoa-10 and 20RM-05, from dominantly Paleoproterozoic to dominantly Cretaceous, unambiguously documenting a shift in provenance polarity, from easterly derived Amazonian cratonic detrital to westerly sourced Andean arc sediments (Figure 10). This shift is further supported by the change from quartzarenites to a rich sedimentary and volcanic lithic sandstones in the same stratigraphic level. Based on previous biostratigraphy and our U–Pb age in the tuffaceous palaeosol of sample 21FL-10, this change occurred at 59.6 + 0.5 Ma in the late Palaeocene. In contrast, in the Florencia area, the coeval Neme Sandstone in the central zone and Palmichal Formation in the northern zone show the dominant source area is Proterozoic Amazon Craton and

13652117, 2025, 3, Downloaded from https://onlinelibrary.wiley.com/doi/10.1111/bre.70041 by Cochrane Colombia, Wiley Online Library on [20/06/2025]. See the Terms and Conditions (https://onlinelibrary.wiley.com/terms-and-conditions) on Wiley Online Library for rules of use; OA articles are governed by the applicable Creative Commons License

Putumayo Basement but minor Palaeozoic zircon U–Pb ages, probably recycled from the Güejar Group. Apatite trace element geochemistry further supports that the Putumayo Basement is the main source (first- order source) area with AUPb age ranges of 1100 Ma to 500 Ma, implying that the Florencia, Macarena and El Melón-Vaupes highs were incipiently uplifted structures that delivered detritus to the northern sector of the basin (Figures 7–9). However, the presence of few Cretaceous zircons suggests an active western source in the Andean arc was already delivering sediment (second-order source) to this basin sector, albeit less so than to the south in the Mocoa area.

The abundance of Cretaceous zircon U–Pb ages in the Rumiyaco Formation in the Mocoa area indicates sources similar to Late Cretaceous plutons such as the Antioquia (99–83 Ma) (Montes et al. 2019), Buga (91 Ma) and Jejenes Batholith (84 Ma) in Colombia (Villagómez et al. 2011; Cardona et al. 2020; Leal-Mejía et al. 2019) that were emplaced in the Central Cordillera at an equatorial latitude (Montes et al. 2019). An alternative source may correspond to the Condúe-Pimampiro Batholith (94–73 Ma) in the Cordillera Real of Ecuador at 0.4° S Lat (Aspden et al. 1992; Gutiérrez et al. 2019). The dominant sedimentary and volcanic lithic composition, together with the few feldspars in sandstone grains in the upper Rumiyaco Formation, indicate that the upper volcanic portion of the arc was the primary sediment source area. The occurrence of metamorphic lithics indicates that the pre-Cretaceous basement of the Central Cordillera was also contributing sedimentary material for this basin. An alternative hypothesis is that some of these Cretaceous zircons may have originated from interbedded volcanic beds in Upper Cretaceous units (De la Parra et al. 2024), which could be considered a second-order source area, similar to what has been previously found in the coeval Napo Formation in the Oriente Basin (Vallejo et al. 2021). The axial and eastern flank of the northern segment (4° N) of the Eastern Cordillera exhibit interbedded volcanic beds within the Cretaceous marine sedimentary cover (Martinez 2010; Ballesteros et al. 2013). These beds were subsequently eroded and transported to the Paleogene foredeeps, increasing the Cretaceous U–Pb signature observed in its synorogenic sediments (Bayona, Baquero, et al. 2020). Moreover, mudstones that are rich in volcanic zircons may significantly influence the U–Pb zircon provenance signature (Sylvester et al. 2022).

The shift of provenance from craton to Andean sources is recorded in coeval stratigraphic units in other northern sub-Andean foreland basins, including the Oriente Basin in Ecuador, the Upper Magdalena Valley Basin in Colombia (Horton 2018; Gutiérrez et al. 2019; Villamizar-Escalante et al. 2021) and southernmost Peruvian basins, such as the Marañon and Huallaga (Louterbach et al. 2018; Hurtado et al. 2018; Custódio et al. 2024). This shift in provenance indicates that the onset of Northern Andean exhumation is in the Late Cretaceous. This exhumation involves Cretaceous granitoids in the Central or Real Cordillera as the first-order source and the unroofing of Cretaceous marine sedimentary cover as a second-order source in the southern area of Mocoa. Additionally, uplifted intraplate basement highs supply detritus to the adjacent northern foredeeps. The earliest record of the Andean exhumation has been documented in other localities. In the Oriente Basin, it was interpreted from provenance proxies as U–Pb detrital ages (Gutiérrez et al. 2019; Martin-Gombojav and Winkler 2008), heavy mineral assemblages (Ruiz 2002; Martin-Gombojav and Winkler 2008) and depositional changes (Christophoul et al. 2002) in the Maastrichtian Tena Formation. A similar approach allowed for the identification of a coeval exhumation episode in the Central Cordillera concurrent with the synorogenic sedimentation of the Upper Magdalena Valley Basin (Gómez et al. 2005; Villamizar-Escalante et al. 2021), the Middle Magdalena Valley Basin (Horton et al. 2010; Valencia-Gómez et al. 2020) and the axial Colombian Eastern Cordillera accompanied by uplift of intraplate basement highs (Bayona, Baquero, et al. 2020).

5.2.2 | Early Eocene Provenance

The Eocene is marked by the deposition of the thick synorogenic sequences of the Pepino Formation (Figure 9C). The Lower Member of the Pepino Formation has a detrital zircon U–Pb age signature like that described for the upper Rumiyaco Formation in the Mocoa area, with abundant Late Cretaceous ages. The sandstone composition, rich in sedimentary and volcanic lithics, is also similar in both units. The Lower Member shows a dominant Upper Cretaceous population with an MDA of 62.0 ± 3.5 Ma in agreement with the Early Eocene biostratigraphic ages (Mora et al. 1998). The high content of sedimentary and volcanic lithics in the sandstones, accompanied by calcareous cement filling the interstitial material, suggests that the Cretaceous sedimentary units (i.e., Olini Group, Villeta Formation) were being unroofed and transported over a relatively short distance. This unroofing occurred through the uplift of southern intraplate basement blocks like those documented in the northern segment of the Eastern Cordillera (Bayona 2018; Bayona, Baquero, et al. 2020; Valencia-Gómez et al. 2020). However, we attribute the dominant Cretaceous detrital zircon U–Pb ages in this lower Eocene sequence to distal Cretaceous plutons in the Central Cordillera or Real Cordillera, in addition to a potential contribution of volcanic zircons from the Upper Cretaceous sedimentary formations.

Nevertheless, the sandstones and conglomerates of the Lower Pepino Formation in the Florencia area have a contrasting composition (Figure 5D). While the sandstones have abundant monocrystalline quartz (70%–80%) and little lithic fragments, whose predominant composition is sedimentary, the conglomerates have abundant chert and sedimentary clasts (~78%), little quartz (2%) and few metamorphic clasts (6%) (Figure 5C). This composition can be explained by a thinner Cretaceous sedimentary cover than in the Mocoa area as the source for these conglomerates, whereas the metamorphic Putumayo basement has been eroded in a larger drainage area feeding the sands with abundant quartz grains (Figure 9C). In adjacent basins, the deposition of an Eocene thick sedimentary section with abundant chert clasts is documented for the Palermo Formation (base of the Gualanday Group) in the Upper Magdalena Valley Basin (Anderson 1972; van Houten and Travis 1968; Caicedo and Roncancio 1994; Bayona et al. 2009; Villamizar-Escalante et al. 2021) and the Lower Member of the Tiyuyaco Formation in the Oriente Basin (Christophoul et al. 2002). Further evidence for contemporaneous sedimentation with the Northern Andean exhumation in these sub-Andean basins derives from the fluvial

13652117, 2025, 3, Downloaded from https://onlinelibrary.wiley.com/doi/10.1111/bre.70041 by Cochrane Colombia, Wiley Online Library on [20/06/2025]. See the Terms and Conditions (https://onlinelibrary.wiley.com/terms-and-conditions) on Wiley Online Library for rules of use; OA articles are governed by the applicable Creative Commons License

paleoflow directions (van Houten and Travis 1968; Christophoul et al. 2002). Southeastward paleocurrents have been identified in the Eocene units such as the Tiyuyacu Formation in the Oriente Basin (Christophoul et al. 2002), the Gualanday Group in the Upper Magdalena Valley Basin (Anderson 1972; van Houten and Travis 1968; Caicedo and Roncancio 1994) and the Pepino Formation in the Putumayo Basin (Mora et al. 1998). Furthermore, unroofing of the Cretaceous sedimentary cover also has been interpreted for the Upper Magdalena Valley Basin from the sediments of the Eocene Gualanday Group related to several episodes of exhumation and basin inversion in the eastern flank of the Central Cordillera through the La Plata–Chuspa Fault system (Villamizar-Escalante et al. 2021).

5.2.3 | Middle—Late Eocene Provenance

In the middle Eocene (~50 Ma), the Middle Member of the Pepino Formation has a detrital U–Pb age signature with no variations in the source in the Mocoa area. Still, its stratigraphic record shows the development of palaeosols and meandering rivers along the foredeep (Figure 9D), suggesting an increase in local accommodation space as indicated by the subsidence curve for this sector (Figure 10).

The Putumayo Basin in the late Eocene is filled with the conglomerates of the Upper Member of the Pepino Formation. This was accompanied by an increase in quartz in the conglomerates and sandstones, while the feldspars and volcanic lithics decreased upsection. The reappearance of the Paleo–Mesoproterozoic U–Pb age populations and the presence of an apatite IM type granitoid LREE signal similar to that found in the Caballos Formation suggest that erosion of this sequence in intraplate highs of the Eastern Cordillera is the main source. In addition, the increase of Palaeozoic and Triassic ages (17%) in the uppermost sample Mocoa-1 suggests erosion of the Triassic–Jurassic Cajamarca Complex and Permian granitoids from the Central Cordillera (Figure 11A; Villagómez and Spikings 2013; Villagómez et al. 2011; Cardona et al. 2010).

In the northern Florencia area, the Upper Pepino Formation has detrital zircon U–Pb age signatures with a large Paleo-Mesoproterozoic population, although the appearance of Norian-Jurassic zircons (10%) in the central zone sample 21FL-03 close to Florencia High, together with apatites sourced by I-type granitoids, suggests that the principal source of this sequence is the Caballos Formation. In the northern zone near the Macarena and El Melón-Vaupes Highs, Proterozoic zircons (20HC-07) and mixed IM, ALK and S apatites suggest that the source was the Putumayo basement. The possible scenario to explain such variation includes a first-order erosion and recycling of the Caballos/Saldaña sequence in both areas with greater involvement of the metamorphic Putumayo basement and recycling of the lower Palaeozoic Güejar Group in the northern zone. The establishment of these basement highs also prevented the advance of middle Eocene marine incursions from the Caribbean farther south of the Llanos Basin (Santos et al. 2008; De La Parra et al. 2021) into the Putumayo Basin (Figure 11B, Santos et al. 2008), the Oriente Basin in Ecuador (Roddaz et al. 2010) and the Huallaga, Santiago and Marañon basins in Peru (Custódio et al. 2023).

5.2.4 | Oligocene-Miocene Provenance

The differences in depositional environments and source areas appear since the early Oligocene, when fluvial and alluvial sediments from the Potrerillo and Doima formations (Gualanday Group) and the base of the late Oligocene Barzalosa Formation continued to be deposited in the Upper Magdalena Valley (Anderson 1972; van Houten and Travis 1968; Caicedo and Roncancio 1994). Fine-grained sediments with marine influence belonging to the Orteguaza Formation were deposited along the foredeep of the Oriente Basin in the late Eocene–early Oligocene (Figure 3; Christophoul et al. 2002; Zambrano et al. 1999) and in the Putumayo Basin in the Oligocene (Figure 9E; Cáceres and Teatin 1985; Govea and Aguilera 1980; Osorio et al. 2002). Similar lacustrine facies of much younger age have been documented at the top of the late early Miocene Barzalosa Formation in the Upper Magdalena Valley Basin (De La Parra et al. 2019) and the early Miocene in the Llanos Basin (Parra et al. 2010; Jaramillo et al. 2017). The provenance for this marine incursion has been proposed from southern Ecuador along the current Guayaquil Gulf into the Amazonian Basin since the Palaeocene (Louterbach et al. 2014) and with a northward path reaching the Putumayo Basin in the late Eocene (Santos et al. 2008).

This marine incursion is interpreted to be driven by an increase in accommodation space generated by an increase in flexural subsidence due to the acceleration of the topographic growth of the Eastern and Central cordilleras. We attribute the increase in topographic load to a change in the subduction configuration, where the former oceanic Farallon Plate tectonic breaks up into the Nazca and Cocos plates at 23 Ma (Figure 11B, González et al. 2023; Somoza 1998). This tectonic reorganisation led to more orthogonal convergence between the newly formed Nazca and South American plates (González et al. 2023). Consequently, the subduction angle of the young and buoyant Nazca Plate shallows (Borrero et al. 2012; Echeverri et al. 2015), modifying mantle wedge flow patterns and generating dynamic subsidence to the east in the Putumayo Basin foredeep (Sacek 2014; Cordeirio-Bicudo et al. 2019; Bicudo et al. 2019; Pachón-Parra et al. 2020; González et al. 2023). Slab shallowing also triggered migration to the east of the magmatic arc in the Western and Central cordilleras (Echeverri et al. 2015) and an increase in their exhumation rates (Villagómez and Spikings 2013). This dynamic subsidence was enhanced and widespread by the middle Miocene when the lacustrine Pebas system was established along the Western Amazon Basin flooding a large part of the basement highs of the Putumayo Basin (Figure 12B, Wesselingh et al. 2002, 2006; Hoorn et al. 2010; Duarte et al. 2017; Jaramillo et al. 2017).

The Miocene Orito Group in the Mocoa area displays increases of quartz, feldspar, metamorphic and volcanic lithics content in sandstones and volcanic clasts in conglomerates that are accompanied by an increase in Cenozoic detrital zircon U–Pb ages, with distinct <40 Ma and Norian-Jurassic arc zircons. In contrast, the detrital U–Pb results for the northern Florencia area reveal more diverse populations (Figures 9F–11A). In the central and northern zones, the basal Orito Group samples show a reversal in provenance polarity, with a switch from cratonic to Andean sources, as also documented in the Campanian-Palaeocene Rumiyaco Formation of the southern Mocoa area. Unlike the

13652117, 2025, 3, Downloaded from https://onlinelibrary.wiley.com/doi/10.1111/bre.70041 by Cochrane Colombia, Wiley Online Library on [20/06/2025]. See the Terms and Conditions (https://onlinelibrary.wiley.com/terms-and-conditions) on Wiley Online Library for rules of use; OA articles are governed by the applicable Creative Commons License

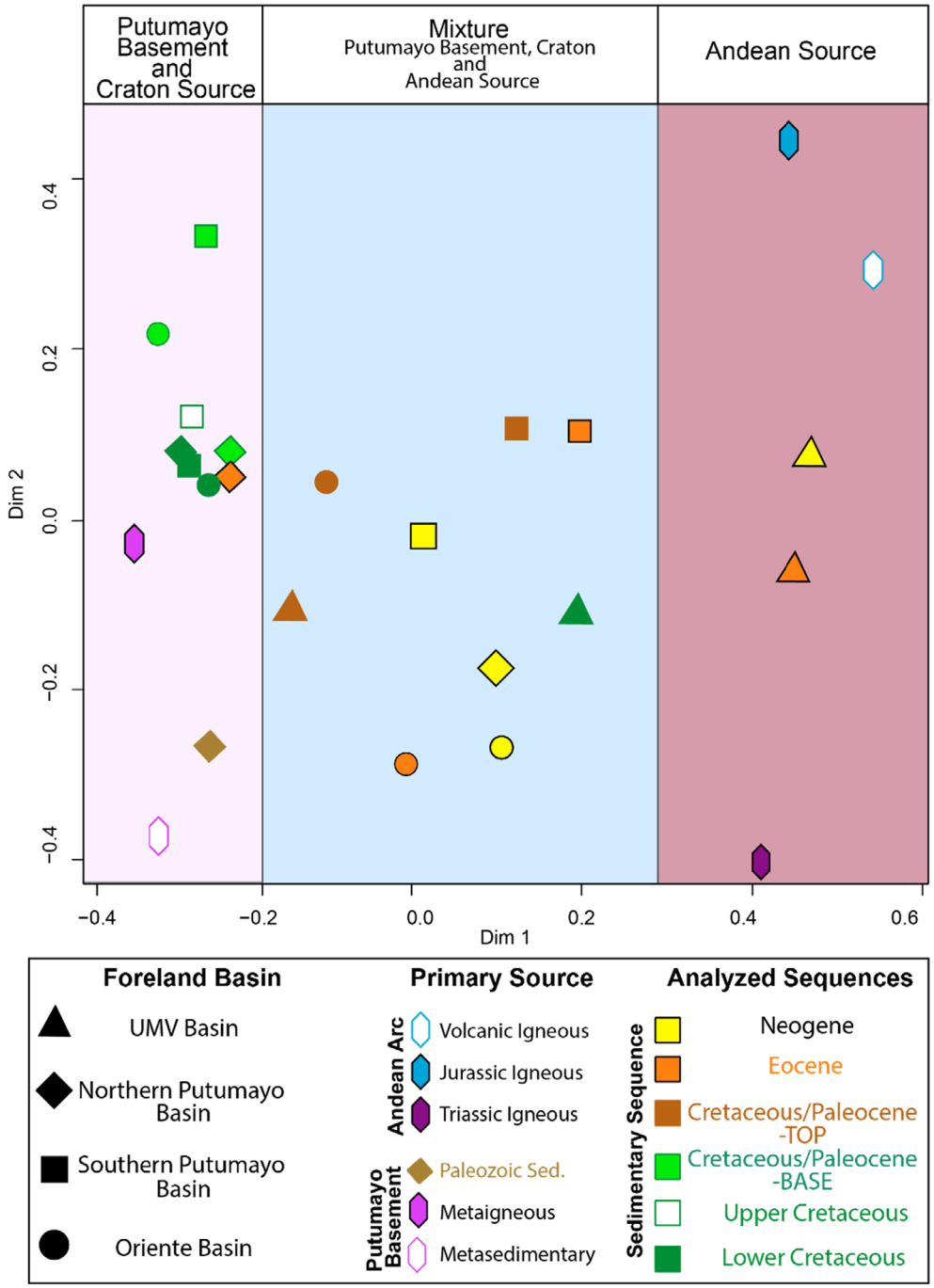

FIGURE 12 | Multidimensional Scaling (MDS) plot for samples from the Oriente (Gutiérrez et al. 2019), Putumayo (this study) and Upper Magdalena Valley (UMV) (Villamizar-Escalante et al. 2021) basins. While the Cretaceous samples show highly similar cratonic provenance across all three basins, the Paleogene and Neogene samples show a dissimilarity that allows them to be placed into two separate provenance fields: either a strictly Andean source or a mixed cratonic with Andean sources.

dominant Cretaceous age populations associated with this switch in the south, in the northern area the dominant ages are Norian-Jurassic and Permo-Triassic. The uppermost samples in both areas have contrasting provenance signatures. While the northern sample shows the reappearance of Mesoproterozoic-Tonian ages, suggesting an exclusive Putumayo basement source, the central sample yields heterogeneous populations with dominant Paleoproterozoic and Mesoproterozoic-Tonian ages, with subordinate Palaeozoic and Permian-Middle Triassic ages, indicating a continued connection with river systems derived from the Central Cordillera. This pattern indicates that unroofing of the Cretaceous cover had ceased and the basin was recording the contribution of multiple sources, mainly from the Putumayo basement (i.e., Garzon Massif), including the recycling of the Palaeozoic sedimentary cover. A second second-order source comprised the pre-Cretaceous crystalline basement and the Neogene plutonic rocks of the Central Cordillera, which will imply a fluvial connection between the Magdalena Valley and the Putumayo basins through a trans-Andean portal, as suggested by Montes et al. (2021). In addition, in the northern

13652117, 2025, 3, Downloaded from https://onlinelibrary.wiley.com/doi/10.1111/bre.70041 by Cochrane Colombia, Wiley Online Library on [20/06/2025]. See the Terms and Conditions (https://onlinelibrary.wiley.com/terms-and-conditions) on Wiley Online Library for rules of use; OA articles are governed by the applicable Creative Commons License

zone, between the Florencia, Macarena and El Melón-Vaupes highs, a unique source from the Putumayo basement suggests that the basin was disconnected from the Central Cordillera, at least since the 10 Ma (Figure 11B). By this time, the tectonic reconstructions document the end of the fragmentation of the Nazca Plate into the Coiba and Malpelo microplates (González et al. 2023). A concomitant steepening of the subduction slab and the development of deep structures such as the Malpelo tear (Idárraga García et al. 2016) could have introduced greater complexity to the mantle wedge flows, consequently leading to heterogeneous subsidence within the Putumayo Basin.

The adjacent Upper Magdalena Valley Basin, located westward of Putumayo Basin and proximal to the Central Cordillera, has a complete record of Miocene sediments cropping out in the Tatacoa Desert at 3° N (Montes et al. 2021). In that place, in addition to the extensive and abundant fossil record (Carrillo et al. 2023 and references therein), the fluvial sandstones of the Honda Group show detrital U–Pb ages with a dominant Cenozoic and Jurassic population (Anderson et al. 2016; Montes et al. 2021), similar to the basal samples of the Orito Group. Miocene strike-slip deformation in the UVM Basin and the Central Cordillera promoted the development of fragmented local sources that feed the drainage system (Zapata et al. 2023), causing heterogeneity in the provenance signals described above. This strike-slip framework occasionally allows for the creation of fluvial passages, which connect the Pacific and Caribbean regions with the Putumayo Basin and may reach the drainage of the Solimoes Formation in the western Amazon (Kern et al. 2020; Zapata et al. 2023).

To better understand how the synorogenic sediments of the Oriente, Putumayo and UVM basins are related to each other in terms of provenance shifts since the late Cretaceous, we divided the population signatures into three main source fields in the MDS plots based on the sample similarity and grouped all samples by chronostratigraphic intervals (Figure 12). For instance, the Pepino samples of the southern zone (20RM-08, 20RM-10, Mocoa-7 and Mocoa-1) are treated as one sample. The craton and basement source field consists of samples with high dominance of a 900 Ma to > 1400 Ma population. A second field corresponds to an Andean source and consists of samples with age predominance in the range < 220 Ma. The third field lies between the former two and represents a combination of the two end-members.

The Cretaceous sequences of Oriente, the northern and southern segments of the Putumayo Basins and even the Palaeozoic rocks from the northern Putumayo Basin have a high affinity with the craton field and suggest an entire basin connected in the Aptian to Campanian times with similar source rocks, except the Upper Magdalena Valley whose Cretaceous sedimentary cover is more related to the Andean source field, which corresponds to rift-shoulders of an extensional, back-arc basin (Sarmiento-Rojas et al. 2006). A similar pattern is identified with individual samples extracted from the same sedimentary sequences (Figure S6). Samples from the base of the Cretaceous/Paleogene sequences (i.e., Rumiyaco Formation) have a high affinity to the craton-basement source throughout the Putumayo Basin. A similar pattern occurs at the top of the Cretaceous/Paleogene sources in the northern Putumayo Basin.

An essential question in the Cenozoic evolution of the northern Andes is when the Central Cordillera started to be exhumed and began contributing detritus to retro-foreland basins (Gómez et al. 2005). The best-documented example is the Middle Magdalena Valley Basin, where provenance analyses, structural/stratigraphic relationships imaged in seismic lines and thermochronological constraints point to a Maastrichtian onset of exhumation (Parra et al. 2012; Nie et al. 2012; Caballero et al. 2013). Our results show that the provenance polarity shift in the Putumayo Basin, from basement rocks of the Putumayo Orogen and Amazonian craton to the Andean magmatic arc, is due to substantial contributions from the uplift and exhumation of the Central Cordillera. In this work, the timing of the initial Andean contribution varies spatially, with sediment input recorded diachronously, with the shift occurring in the Maastrichtian south of the Putumayo Basin, in the late Eocene at the latitude of the Florencia High and finally in the early Miocene at the latitude of the Macarena and El Melón-Vaupes Highs (Figures 6 and 7).

Our MDS plot shows how the affinity of the sediments becomes closer to an Andean arc source (Figure 12). Within the UVM Basin, the Lower Cretaceous succession is positioned closer to this region, while the Eocene sequence is undeniably associated with it. While in southern Putumayo, the closest sequences to this field are the upper part of the late Cretaceous/Palaeocene sequence and the Neogene sequences in northern Putumayo. This tendency suggests a northward diachroneity related to a differential uplift of the Central Cordillera. Further, in the Oriente Basin, the Neogene succession exhibits a major affinity to the Andean magmatic arc, which reflects a Late Cretaceous through Cenozoic trend toward greater arc material.

This multi-proxy approach shows that the Putumayo and Oriente basins record a wholesale shift in provenance polarity from cratonic to Andean sources, where Campanian-Maastrichtian (72–65 Ma) strata record the initial exhumation of the Eastern Cordillera of southern Colombia (this study) and the Cordillera Real of Ecuador (Martin-Gombojav and Winkler 2008; Horton 2018; Gutiérrez et al. 2019). In addition, the progressive cratonward advance of exhumation during the Eocene (59–34 Ma)—as expressed in the fold-thrust belts flanking these basins and/or in intrabasinal structural highs—triggered erosional recycling of Cretaceous cover strata and deposition of proximal alluvial fan conglomerates in local depocenters within a broken foreland configuration. Finally, Miocene strike-slip deformation and dynamic subsidence (Sacek 2014; Cordeirio-Bicudo et al. 2019) may have further influenced foreland deposition with a heterogeneous distribution of source rocks associated with multiple marine incursions.

5.3 | Regional Tectonic Implications

The new findings bearing on sediment provenance and basin evolution provide a new paleogeographic perspective for the Northern Andean configuration concerning the early exhumation of both the Central Cordillera and Eastern Cordillera during the Late Cretaceous through Cenozoic (Figure 11). The Putumayo Basin of southern Colombia records the evolution

13652117, 2025, 3, Downloaded from https://onlinelibrary.wiley.com/doi/10.1111/bre.70041 by Cochrane Colombia, Wiley Online Library on [20/06/2025]. See the Terms and Conditions (https://onlinelibrary.wiley.com/terms-and-conditions) on Wiley Online Library for rules of use; OA articles are governed by the applicable Creative Commons License

of a Cenozoic broken foreland basin filled with thick synorogenic clastic deposits affected both by thrust belt development in the west and uplift of basement highs within the basin itself. Evidence for intraplate uplift comes from stratigraphic thinning of synorogenic strata toward several large-wavelength structural highs. During the Late Cretaceous, tectonic events such as the oblique collision of the Caribbean Large Igneous Province (CLIP) oceanic plateau against the continental South American Plate (Figure 10) (McCourt et al. 1984; Kerr et al. 1996; Vallejo et al. 2006, 2009; Jaillard et al. 2009; Cardona et al. 2011; Montes et al. 2019) helped trigger early exhumation of the Central Cordillera in Colombia (Villagómez and Spikings 2013) and the Cordillera Real in Ecuador (Spikings et al. 2001, 2010; Vallejo et al. 2006; Spikings and Simpson 2014). Increased exhumation rates during the Campanian-Maastrichtian (80–70 Ma) have been documented through thermochronometry of Jurassic granitoids such as the Ibague Batholith in the Central Cordillera (Villagomez 2010; Villagómez and Spikings 2013) or the Azafran Granite in the Real Cordillera (Spikings et al. 2000). Phenomena associated with this CLIP collision, such as crustal thickening in Ecuador (George et al. 2021) or the establishment of a protracted magmatic arc with a paleoelevation of ~2 km within the Central Cordillera of Colombia (León et al. 2021) characterise the evolving tectonic configuration for the northern Andes during the Cenozoic. Numerical models show the development of different subduction geometries during the collision of CLIP with the South American Plate, including the initial flat slab subduction (Riel et al. 2023).

Perhaps the most characteristic signature of this early Andean collision involves inboard deformation within the Eastern Cordillera, as manifest in the uplift of intraplate basement highs that influenced sedimentation patterns in the foreland basin, as shown by provenance changes in the southern Llanos Basin, the axial zone of Eastern Cordillera (Bayona, Baquero, et al. 2020; Bayona 2018), the Oriente Basin of Ecuador (Gutiérrez et al. 2019; Vallejo et al. 2021) and our current findings for the Putumayo Basin of southern Colombia (Figure 12). In addition, the development of additional intraplate highs farther north within the Eastern Cordillera was triggered by the flat slab subduction that also produced the latest Palaeocene intraplate magmatic activity recorded as far east as in the adjacent Llanos Basin (Bayona et al. 2012, 2013, 2015; Bayona 2018).

Numerical modelling has shown that when a buoyant oceanic plateau collides with a thick continental lithosphere that moves rapidly trenchward, a common scenario involves the development of flat slab subduction and therefore shortening and uplift far inboard of the trench (Liu and Currie 2019). Similar to the well-documented Laramide Orogeny in North America (Liu et al. 2010; Lawton 2019 and references therein), we propose that the infilling of the Putumayo Basin in the latest Cretaceous to Cenozoic was influenced by the uplift of basement structures associated with thick-skinned deformation along the Garzón Massif (Saeid et al. 2017; Wolaver et al. 2015) in a broken foreland configuration with erosional unroofing of sedimentary cover from basement-involved highs, as documented for the North American Laramide Orogeny (Yonkee and Weil 2015; Lawton 2019; Horton et al. 2022).

6 | Conclusions

The exhumation of the Northern Andes, particularly the southern segment of the Eastern Cordillera, began during the Late Cretaceous period when the Caribbean Plate collided obliquely with the South American Plate. The provenance signals in the sediments deposited in the Putumayo Basin provide evidence of this event. The orogenic growth facilitated the establishment of a broken foreland basin, resulting in the uplift of intraplate highs as those in the northern sector of the basin due to the flat slab subduction of CLIP. This process is similar to that documented in the Laramide Orogeny in North America (Lawton 2019 and references therein).

The configuration of the broken foreland basin during the Cenozoic influenced the provenance signatures and facies distribution along the foredeep of the Putumayo Basin. The southern foredeep (Mocoa area) was dominated by meandering rivers and palaeosols during the Late Cretaceous and Paleogene. In contrast, the northern foredeep (Florencia area) has thick sequences of sandstones in fluvial-deltaic environments conditioned by the Florencia, Macarena and El Melón-Vaupes intraplate highs. The change in sandstone composition and detrital zircon U–Pb signature polarity, from Amazonian craton to Andean sources in the Rumiyaco Formation, confirms the onset of Late Cretaceous exhumation in the Central Cordillera as a primary source area, as well as the coeval incipient exhumation of the Eastern Cordillera as isolated intraplate uplifts as a secondary source area. The less prominent change in provenance signatures in the northern foredeep can be explained by the exposure of the basement as an intraplate high, which promotes the unconformable deposition of a sequence of locally condensed sandstones (i.e., Neme Sandstone).

The Eocene synorogenic succession was deposited in fluvial and alluvial fan environments. The provenance signatures and composition of the sandstones and conglomerates indicate ongoing exhumation of the Central Cordillera to the south that began in the Late Cretaceous, allowing for the unroofing of the sedimentary cover overlying the Putumayo basement and the local erosion of the basement itself in the Florencia and Macarena, and El Melón–Vaupes intraplate highs, accompanied by the Central Cordillera as a second-order source area. In contrast, the sedimentary provenance and facies distribution of the Orito Group during the Oligocene–Miocene period were more heterogeneous, including an increase in accommodation space due to an increase in flexural subsidence enhanced by dynamic subsidence resulting from the tectonic reorganisation of the subducting plates to the west. The increase in subsidence is associated with the Oligocene breakup of the Farallon Plate into the more orthogonally convergent Nazca Plate in the south and the Cocos Plate in the north. A more complex subsidence pattern resulted from the Middle Miocene breakup of the northern Nazca Plate into the Malpelo and Coiba microplates. This is reflected in the deposition of grey mudstone facies in lacustrine environments with marine influence during the Oligocene. In the Miocene, the depositional environment changed to fluvial, with the development of palaeosols. The provenance signature of the Orito Group is heterogeneous due to a strike-slip configuration of the Northern Andes triggering the reorganisation of

13652117, 2025, 3, Downloaded from https://onlinelibrary.wiley.com/doi/10.1111/bre.70041 by Cochrane Colombia, Wiley Online Library on [20/06/2025]. See the Terms and Conditions (https://onlinelibrary.wiley.com/terms-and-conditions) on Wiley Online Library for rules of use; OA articles are governed by the applicable Creative Commons License

several sediment source areas, as also recorded in the Oriente Basin in Ecuador. The foredeep deposits there also document the onset of the exhumation of the Northern Andes during the Late Cretaceous (Gutiérrez et al. 2019).

In contractional orogenic systems, the transition from sag basin to retro-foreland basin is characterised by continuous deposition of sediments in a broad depocenter, resulting from the flexure of the upper plate. Our findings indicate that this transition in the Putumayo Basin is marked by the early uplift of basement highs of an incipient Eastern Cordillera during the flexural stage, which disrupts the depositional systems and influences the provenance of synorogenic deposits typical of a broken foreland basin.

Acknowledgements

This project is part of the FAPESP JP2 Project 2018/15613-1 "Topographic Construction along the northern Andes and the Origin of the transcontinental Amazon River" and CNPq grant PQ 307324/2022-2 to M.P. We are grateful to Ecopetrol S.A for allowing publication of apatite U–Pb REE data. G.N. is funded by the Human Resources Petroleum Program 43.1, financed by the Brazilian National Agency for Petroleum, Natural Gas and Biofuels (ANP). B.K.H. is financed by the US National Science Foundation grants EAR-1925939 and EAR-1925898. A.C. was supported by project HERMES 61057 from the National University of Colombia. Constructive comments by an anonymous reviewer and German Bayona, and Associate Editor Sarah Falkowski helped improve the content of this manuscript. The Article Processing Charge for the publication of this research was funded by the Coordenação de Aperfeiçoamento de Pessoal de Nível Superior - Brasil (CAPES) (ROR identifier: 00x0ma614).

Conflicts of Interest

The authors declare no conflicts of interest.

Data Availability Statement

The data sets used and/or analyzed during the current study are available from the corresponding author on reasonable request.

Peer Review

The peer review history for this article is available at https://www.webofscience.com/api/gateway/wos/peer-review/10.1111/bre.70041.

References

Anderson, T. A. 1972. "Paleogene Nonmarine Gualanday Group, Neiva Basin, Colombia, and Regional Development of the Colombian Andes." *Geological Society of America Bulletin* 83, no. 8: 2423–2438.

Anderson, V. J., B. H. Horton, J. E. Saylor, et al. 2016. "Andean Topographic Growth and Basement Uplift in Southern Colombia: Implications for the Evolution of the Magdalena, Orinoco, and Amazon River Systems." *Geosphere* 12, no. 4: 1235–1256.

ANH-UPTC. 2009. "Cartografía Geológica de 5167.45 Km2 en la Cuenca Caguan-Putumayo a Partir de Sensores Remotos a Escala 1:100000 y 739 Km2 con Control de Campo a Escala 1:50000 en las Planchas IGAC 413 y 414." Departamentos de Meta, Caquetá y Putumayo. 111 p.

Antonelli, A., J. A. Nylander, C. Persson, and I. Sanmartín. 2009. "Tracing the Impact of the Andean Uplift on Neotropical Plant Evolution." *Proceedings of the National Academy of Sciences of the United States of America* 106, no. 24: 9749–9754.

Aspden, J. A., S. H. Harrison, and C. C. Rundle. 1992. "New Geochronological Control for the Tectono-Magmatic Evolution of the Metamorphic Basement, Cordillera Real and El Oro Province of Ecuador." *Journal of South American Earth Sciences* 6, no. 1–2: 77–96.

Baby, P., M. Rivadeneira, R. Barragán, and F. Christophoul. 2013. "Thick-Skinned Tectonics in the Oriente Foreland Basin of Ecuador." *Geological Society, London, Special Publications* 377, no. 1: 59–76.

Baker, P. A., S. C. Fritz, C. W. Dick, et al. 2014. "The Emerging Field of Geogenomics: Constraining Geological Problems With Genetic Data." *Earth-Science Reviews* 135: 38–47. https://doi.org/10.1016/j.earscirev.2014.04.001.

Ballesteros, C. I., H. A. Galvis, I. C. Higuera, et al. 2013. "Anotaciones Acerca de la Estratigrafía del Intervalo Cenomaniano-Campaniano Atravesado por el pozo La Luna-1, Cuenca del Valle Medio del Magdalena." XVI Congreso Colombiano de Geología, Bogotá, p. 30–31.

Barbosa-Espitia, Á. A., G. D. Kamenov, D. A. Foster, S. A. Restrepo-Moreno, and A. Pardo-Trujillo. 2019. "Contemporaneous Paleogene Arc-Magmatism Within Continental and Accreted Oceanic Arc Complexes in the Northwestern Andes and Panama." *Lithos* 348: 105185.

Bayona, G. 2018. "El Inicio de la Emergencia en los Andes del Norte: una Perspectiva a Partir del Registro Tectónico-Sedimentológico del Coniaciano al Paleoceno." *Revista de la Academia Colombiana de Ciencias Exactas, Físicas y Naturales* 42, no. 165: 364–378.

Bayona, G., M. Baquero, C. Ramírez, et al. 2020. "Unravelling the Widening of the Earliest Andean Northern Orogen: Maastrichtian to Early Eocene Intra-Basinal Deformation in the Northern Eastern Cordillera of Colombia." *Basin Research* 33, no. 1: 809–845.

Bayona, G., C. Bustamante, G. Nova, and A. M. Salazar–Franco. 2020. "Jurassic Evolution of the Northwestern Corner of Gondwana: Present Knowledge and Future Challenges in Studying Colombian Jurassic Rocks." In *The Geology of Colombia, Volume 2 Mesozoic*, edited by J. Gómez and A. O. Pinilla–Pachon, 37. Servicio Geológico Colombiano, Publicaciones Geológicas Especiales 36. https://doi.org/10.32685/pub.esp.36.2019.05.

Bayona, G., A. Cardona, C. Jaramillo, et al. 2013. "Onset of Fault Reactivation in the Eastern Cordillera of Colombia and Proximal Llanos Basin; Response to Caribbean–South American Convergence in Early Palaeogene Time." *Geological Society, London, Special Publications* 377, no. 1: 285–314.

Bayona, G., A. Cardona, C. Jaramillo, et al. 2012. "Early Paleogene Magmatism in the Northern Andes: Insights on the Effects of Oceanic Plateau–Continent Convergence." *Earth and Planetary Science Letters* 331: 97–111.

Bayona, G., A. Cardona, G. Tellez, et al. 2015. "Magmatismo Paleoceno-Eoceno Temprano (?) en la Cuenca Proximal de los Llanos." In XV Congreso Colombiano de Geología, Bucaramanga, Colombia, 560–563.

Bayona, G., M. Cortés, C. Jaramillo, G. Ojeda, J. J. Aristizabal, and A. Reyes-Harker. 2008. "An Integrated Analysis of an Orogen–Sedimentary Basin Pair: Latest Cretaceous–Cenozoic Evolution of the Linked Eastern Cordillera Orogen and the Llanos Foreland Basin of Colombia." *Geological Society of America Bulletin* 120, no. 9–10: 1171–1197.

Bayona, G., D. F. García, and G. Mora. 1994. "La Formación Saldaña: Producto de la Actividad de Estratovolcanes Continentales en un Dominio de Retroarco." In *Estudios Geológicos del Valle Superior del Magdalena*, edited by F. Etayo-Serna, I–1–1–21. Universidad Nacional de Colombia–Ecopetrol.

Bayona, G., F. Lamus, G. Jimenez, et al. 2009. "Conteo de Clastos Como Metodologia en el Reconocimiento de Unidades Conglomeraticas en el Valle Superior del Magdalena (VSM)." XII Congreso Colombiano de Geología, Paipa, Colombia.

Beltrán, W., W. Espitia, D. Bello-Palacios, J. Arias, and I. C. H. Díaz. 2022. "Structural Styles of the Southern Putumayo Foreland Basin,

13652117, 2025, 3, Downloaded from https://onlinelibrary.wiley.com/doi/10.1111/bre.70041 by Cochrane Colombia, Wiley Online Library on [20/06/2025]. See the Terms and Conditions (https://onlinelibrary.wiley.com/terms-and-conditions) on Wiley Online Library for rules of use; OA articles are governed by the applicable Creative Commons License

Northern Andes, Colombia." In *Andean Structural Styles*, 227–234. Elsevier.

Bicudo, T. C., V. Sacek, R. P. de Almeida, J. M. Bates, and C. C. Ribas. 2019. "Andean Tectonics and Mantle Dynamics as a Pervasive Influence on Amazonian Ecosystem." *Scientific Reports* 9, no. 1: 16879. https://doi.org/10.1038/s41598-019-53465-y.

Blanco-Quintero, I. F., A. García-Casco, L. M. Toro, et al. 2014. "Late Jurassic Terrane Collision in the Northwestern Margin of Gondwana (Cajamarca Complex, Eastern Flank of the Central Cordillera, Colombia)." *International Geology Review* 56, no. 15: 1852–1872.

Black, L. P., S. L. Kamo, C. M. Allen, et al. 2004. "Improved 206Pb/238U Microprobe Geochronology by the Monitoring of a Trace-Element-Related Matrix Effect; SHRIMP, ID–TIMS, ELA–ICP–MS and Oxygen Isotope Documentation for a Series of Zircon Standards." *Chemical Geology* 205, no. 1–2: 115–140.

Borrero, C., A. Pardo, C. M. Jaramillo, et al. 2012. "Tectonostratigraphy of the Cenozoic Tumaco Forearc Basin (Colombian Pacific) and Its Relationship With the Northern Andes Orogenic Build Up." *Journal of South American Earth Sciences* 39: 75–92.

Buchely, F., L. Gomez, J. Buitrago, et al. 2015. *Elaboración de la Cartografía Geológica de un Conjunto de Planchas a Escala 1:100000 Ubicadas en Cuatro Bloques del Territorio Nacional Identificados Por el Servicio Geológico Colombiano Srupo 2: Zonas Sur A y Zona Sur B*, 127. Geología de la Plancha 413-Florencia.

Bustamante, C., C. J. Archanjo, A. Cardona, A. Bustamante, and V. A. Valencia. 2017. "U-Pb Ages and Hf Isotopes in Zircons From Parautochthonous Mesozoic Terranes in the Western Margin of Pangea: Implications for the Terrane Configurations in the Northern Andes." *Journal of Geology* 125, no. 5: 487–500.

Bustamante, C., C. J. Archanjo, A. Cardona, and J. D. Vervoort. 2016. "Late Jurassic to Early Cretaceous Plutonism in the Colombian Andes: A Record of Long-Term Arc Maturity." *Bulletin* 128, no. 11–12: 1762–1779.

Bustamante, C., A. Cardona, C. J. Archanjo, G. Bayona, M. Lara, and V. Valencia. 2017. "Geochemistry and Isotopic Signatures of Paleogene Plutonic and Detrital Rocks of the Northern Andes of Colombia: A Record of Post-Collisional Arc Magmatism." *Lithos* 277: 199–209.

Caballero, V., A. Mora, I. Quintero, et al. 2013. "Tectonic Controls on Sedimentation in an Intermontane Hinterland Basin Adjacent to Inversion Structures: The Nuevo Mundo Syncline, Middle Magdalena Valley, Colombia." *Geological Society, London, Special Publications* 377, no. 1: 315–342.

Cáceres, H., and P. Teatin. 1985. "Cuenca del Putumayo, provincia petrolífera meridional de Colombia." In *2nd Simposio Bolivariano Exploracion Petrolera en las Cuencas Subandinas*. (91 p) Extended Abstracts.

Caicedo, J. C., and J. Roncancio. 1994. "El Grupo Gualanday Como Ejemplo de Acumulación Sintectónica, en el Valle Superior del Magdalena, Durante el Paleógeno." In *Estudios Geológicos del Valle Superior del Magdalena, Capitulo X* (Fernando Etayo-Serna., 1-19). Universidad Nacional de Colombia, Facultad de ciencias.

Calderon-Diaz, L., S. Zapata, A. Cardona, et al. 2024. "Cretaceous Extensional and Contractional Stages in the Colombian Andes Unraveled by a Source-to-Sink Geochronological and Thermochronological Study in the Upper Magdalena Basin." *Tectonophysics* 878: 230303.

Calvet, M., M. Delmas, Y. Gunnell, and B. Laumonier. 2022. "Basin Analysis: The Sedimentary Record of Orogenic Growth and Decay." In *Geology and Landscapes of the Eastern Pyrenees: A Field Guide With Excursions*, 27–56. Springer International Publishing.

Cardona, A., U. G. Cordani, J. Ruiz, et al. 2009. "U-Pb Zircon Geochronology and Nd Isotopic Signatures of the Pre-Mesozoic Metamorphic Basement of the Eastern Peruvian Andes: Growth and Provenance of a Late Neoproterozoic to Carboniferous Accretionary Orogen on the Northwest Margin of Gondwana." *Journal of Geology* 117: 285–305. https://doi.org/10.1086/597472.

Cardona, A., S. León, J. S. Jaramillo, et al. 2018. "The Paleogene Arcs of the Northern Andes of Colombia and Panama: Insights on Plate Kinematic Implications From New and Existing Geochemical, Geochronological and Isotopic Data." *Tectonophysics* 749: 88–103.

Cardona, A., V. A. Valencia, G. Bayona, et al. 2011. "Early-Subduction-Related Orogeny in the Northern Andes: Turonian to Eocene Magmatic and Provenance Record in the Santa Marta Massif and Rancheria Basin, Northern Colombia." *Terra Nova* 23, no. 1: 26–34.

Cardona, A., V. Valencia, A. Garzon, et al. 2010. "Permian to Triassic I to S-Type Magmatic Switch in the Northeast Sierra Nevada de Santa Marta and Adjacent Regions, Colombian Caribbean: Tectonic Setting and Implications Within Pangea Paleogeography." *Journal of South American Earth Sciences* 29: 772–783.

Cardona, A., S. León, J. S. Jaramillo, et al. 2020. "Cretaceous Record From a Mariana to an Andean–Type Margin in the Central Cordillera of the Colombian Andes." In *The Geology of Colombia, Volume 2 Mesozoic*, edited by J. Gómez and A. O. Pinilla-Pachon, vol. 36, 335–373. Servicio Geológico Colombiano, Publicaciones Geológicas Especiales. Bogotá.

Carrillo, J. D., C. Jaramillo, F. Abadía, et al. 2023. "The Miocene La Venta Biome (Colombia): A Century of Research and Future Perspectives." *Geodiversitas* 45, no. 26: 739–767.

Cediel, F., J. Mojica, and C. Macia. 1981. "Las Formaciones Luisa, Payandé y Saldaña sus Columnas Estratigraficas Características." *Geología Norandina* 3: 11–19.

Chang, Z., J. D. Vervoort, W. C. McClelland, and C. Knaack. 2006. "U-Pb Dating of Zircon by LA-ICP-MS." *Geochemistry, Geophysics, Geosystems* 7, no. 5: 1–14.

Chavarría, L., C. Bustamante, A. Cardona, and G. Bayona. 2022. "Quantifying Crustal Thickness and Magmatic Temperatures of the Jurassic to Early Cretaceous North-Andean arc." *International Geology Review* 64, no. 18: 2544–2564.

Chew, D. M., R. A. Donelick, and P. Sylvester. 2012. "Combined Apatite Fission Track and U-Pb Dating by LA-ICP-MS and Its Application in Apatite Provenance Analysis." In *Quantitative Mineralogy and Microanalysis of Sediments and Sedimentary Rocks: Mineralogical Association of Canada, Short Course*, edited by P. Sylvester 42, 219–247. Mineralogical Association of Canada.

Chew, D. M., J. A. Petrus, and B. S. Kamber. 2014. "U-Pb LA–ICPMS Dating Using Accessory Mineral Standards With Variable Common Pb." *Chemical Geology* 363: 185–199.

Chew, D. M., M. G. Babechuk, N. Cogne, et al. 2016. "(LA, Q)-ICPMS Trace-Element Analyses of Durango and McClure Mountain Apatite and Implications for Making Natural LA-ICPMS Mineral Standards." *Chemical Geology* 435: 35–48.

Christophoul, F., P. Baby, and C. Dávila. 2002. "Stratigraphic Responses to a Major Tectonic Event in a Foreland Basin: The Ecuadorian Oriente Basin From Eocene to Oligocene Times." *Tectonophysics* 345, no. 1–4: 281–298.

Cochrane, R., R. A. Spikings, D. Chew, et al. 2014. "High Temperature (> 350 C) Thermochronology and Mechanisms of Pb Loss in Apatite." *Geochimica et Cosmochimica Acta* 127: 39–56.

Cochrane, R., R. Spikings, A. Gerdes, et al. 2014. "Permo-Triassic Anatexis, Continental Rifting and the Disassembly of Western Pangaea." *Lithos* 190: 383–402.

Cooper, M. A., F. T. Addison, R. Alvarez, et al. 1995. "Basin Development and Tectonic History of the Llanos Basin, Eastern Cordillera, and Middle Magdalena Valley, Colombia." *AAPG Bulletin* 79: 1421–1443.

Copeland, P. 2020. "On the Use of Geochronology of Detrital Grains in Determining the Time of Deposition of Clastic Sedimentary Strata." *Basin Research* 32, no. 6: 1532–1546.

13652117, 2025, 3, Downloaded from https://onlinelibrary.wiley.com/doi/10.1111/bre.70041 by Cochrane Colombia, Wiley Online Library on [20/06/2025]. See the Terms and Conditions (https://onlinelibrary.wiley.com/terms-and-conditions) on Wiley Online Library for rules of use; OA articles are governed by the applicable Creative Commons License

Cordani, U. G., A. Cardona, D. M. Jimenez, D. Liu, and A. P. Nutman. 2005. "Geochronology of Proterozoic Basement Inliers in the Colombian Andes: Tectonic History of Remnants of a Fragmented Grenville Belt." *Geological Society of London, Special Publication* 246: 329–346. https://doi.org/10.1144/GSL.SP.2005.246.01.13.

Cordani, U. G., and W. Teixeira. 2007. "Proterozoic Accretionary Belts in the Amazonian Craton." In *Geological Society of America Memoirs*, 297–320. Geological Society of America.

Cordeirio-Bicudo, T., V. Sacek, and R. P. de Almeida. 2019. "Reappraisal of the Relative Importance of Dynamic Topography and Andean Orogeny on Amazon Landscape Evolution." *Earth and Planetary Science Letters* 546: 116423.

Corredor, F., N. Piragauta, N. Delgado, A. Cifuentes, and J. Palencia. 2019. "Active Reverse Faulting During the Late Cretaceous-Early Tertiary in the Putumayo Basin, Colombia: Implications for the Exploration of Hydrocarbons." Abstract Extended, I Cumbre del Petroleo & Gas, Noviembre 14–18, Bogotá, Colombia.

Custódio, M. A., M. Roddaz, R. V. Santos, et al. 2023. "New Stratigraphic and Paleoenvironmental Constraints on the Paleogene Paleogeography of Western Amazonia." *Journal of South American Earth Sciences* 124: 104256.

Custódio, M. A., M. Roddaz, R. V. Santos, et al. 2024. "Maastrichtian-Cenozoic Erosional History of the Northern Peruvian Amazonian Andes Implications for the Eastern Cordillera Evolution (Huallaga Basin, Northern Peru)." *Global and Planetary Change* 242: 104584.

De la Parra, F., C. Higuera, R. Ramírez, et al. 2024. "Chronostratigraphy of the Upper Cretaceous Succession in the Middle Magdalena Valley of Colombia (Northern South America)." *Cretaceous Research* 157: 105824.

De La Parra, F., D. Pinzon, F. Mantilla-Duran, G. Rodriguez, and V. Caballero. 2021. "Marine-Lacustrine Systems During the Eocene in Northern South America–Palynological Evidence From Colombia." *Journal of South American Earth Sciences* 108: 103188.

De La Parra, F., D. Pinzon, G. Rodriguez, O. Bedoya, and R. Benson. 2019. "Lacustrine Systems in the Early Miocene of Northern South America—Evidence From the Upper Magdalena Valley, Colombia." *PALAIOS* 34, no. 10: 490–505.

DeCelles, P. G., B. Carrapa, B. K. Horton, and G. E. Gehrels. 2011. "Cenozoic Foreland Basin System in the Central Andes of Northwestern Argentina: Implications for Andean Geodynamics and Modes of Deformation." *Tectonics* 30, no. 6: 1–30. https://doi.org/10.1029/2011TC002948.

DeCelles, P. G., G. E. Gehrels, J. Quade, T. P. Ojha, P. A. Kapp, and B. N. Upreti. 1998. "Neogene Foreland Basin Deposits, Erosional Unroofing, and the Kinematic History of the Himalayan Fold-Thrust Belt, Western Nepal." *Geological Society of America Bulletin* 110: 2–21.

Dickinson, W. R. 1985. "Interpreting Provenance Relations From Detrital Modes of Sandstones." In *Provenance of Arenites*, edited by G. G. Zuffa, 333–361. Springer.

Dickinson, W. R., L. S. Beard, G. R. Brakenridge, et al. 1983. "Provenance of North American Phanerozoic Sandstones in Relation to Tectonic Setting." *Geological Society of America Bulletin* 94, no. 2: 222–235.

Dickinson, W. R., and C. A. Suczek. 1979. "Plate Tectonics and Sandstone Composition." *American Association of Petroleum Geologists Bulletin* 63: 2164–2182.

Duarte, E., G. Bayona, C. Jaramillo, M. Parra, I. Romero, and J. A. Mora. 2017. "Identificación de los máximos eventos de inundación marina Miocenos y su uso en la correlación y análisis de la cuenca de antepaís de los Llanos Orientales, Colombia." *Boletín de Geología* 39, no. 1: 19–40.

Echeverri, S., A. Cardona, A. Pardo, et al. 2015. "Regional Provenance From Southwestern Colombia Fore-Arc and Intra-Arc Basins: Implications for Middle to Late Miocene Orogeny in the Northern Andes." *Terra Nova* 27, no. 5: 356–363.

Etayo-Serna, F. 1994. "A Modo de Historia Geológica del Cretácico en el Valle Superior del Magdalena." In *Estudios Geológicos del Valle Superior del Magdalena, Capítulo XX*, edited by F. Etayo-Serna, 1–5. Universidad Nacional de Colombia, Facultad de ciencias.

Folguera, A., G. Bottesi, I. Duddy, et al. 2015. "Exhumation of the Neuquén Basin in the Southern Central Andes (Malargüe Fold and Thrust Belt) From Field Data and Low-Temperature Thermochronology." *Journal of South American Earth Sciences* 64: 381–398.

Folk, R. L. 1980. *Petrology of Sedimentary Rocks*. Hemphill Publishing Company.

Gallagher, K. 2012. "Uplift, Denudation, and Their Causes and Constraints Over Geological Timescales." In *Regional Geology and Tectonics: Principles of Geologic Analysis*, edited by D. G. Roberts and A. W. Bally, 609–644. Elsevier.

Garzanti, E. 2016. "From Static to Dynamic Provenance Analysis—Sedimentary Petrology Upgraded." *Sedimentary Geology* 336: 3–13.

Garzanti, E., C. Doglioni, G. Vezzoli, and S. Ando. 2007. "Orogenic Belts and Orogenic Sediment Provenance." *Journal of Geology* 115, no. 3: 315–334.

Garzanti, E., and M. G. Malusà. 2008. "The Oligocene Alps: Domal Unroofing and Drainage Development During Early Orogenic Growth." *Earth and Planetary Science Letters* 268, no. 3–4: 487–500.

Garzione, C. N., N. McQuarrie, N. D. Perez, et al. 2017. "The Tectonic Evolution of the Central Andean Plateau and Geodynamic Implications for the Growth of Plateaus." *Annual Review of Earth and Planetary Sciences* 45: 529–559. https://doi.org/10.1146/annurev-earth-063016-020612.

Gehrels, G. 2014. "Detrital Zircon U-Pb Geochronology Applied to Tectonics." *Annual Review of Earth and Planetary Sciences* 42: 127–149.

Gehrels, G., and M. Pecha. 2014. "Detrital Zircon U-Pb Geochronology and Hf Isotope Geochemistry of Paleozoic and Triassic Passive Margin Strata of Western North America." *Geosphere* 10, no. 1: 49–65.

Gehrels, G., V. Valencia, and A. Pullen. 2006. "Detrital Zircon Geochronology by Laser Ablation Multicollector ICPMS at the Arizona LaserChron Center." In *Geochronology Emerging Opportunities*, edited by T. D. Olszewski, vol. 12, 67–76. Paleontological Society.

Gehrels, G. E., V. A. Valencia, and J. Ruiz. 2008. "Enhanced Precision, Accuracy, Efficiency, and Spatial Resolution of U-Pb Ages by Laser Ablation–Multicollector–Inductively Coupled Plasma–Mass Spectrometry." *Geochemistry, Geophysics, Geosystems* 9, no. 3: 1–13.

George, S. W., B. K. Horton, C. Vallejo, L. J. Jackson, and E. G. Gutierrez. 2021. "Did Accretion of the Caribbean Oceanic Plateau Drive Rapid Crustal Thickening in the Northern Andes?" *Geology* 49, no. 8: 936–940.

Gómez, E., T. E. Jordan, R. W. Allmendinger, K. Hegarty, and S. Kelley. 2005. "Syntectonic Cenozoic Sedimentation in the Northern Middle Magdalena Valley Basin of Colombia and Implications for Exhumation of the Northern Andes." *Geological Society of America Bulletin* 117, no. 5–6: 547–569.

González, R., O. Oncken, C. Faccenna, E. Le Breton, M. Bezada, and A. Mora. 2023. "Kinematics and Convergent Tectonics of the Northwestern South American Plate During the Cenozoic." *Geochemistry, Geophysics, Geosystems* 24, no. 7: e2022GC010827.

Govea, C., and H. Aguilera. 1980. "Geología de la Cuenca del Putumayo." *Boletín de Geología* 14, no. 28: 45–71.

Guerrero, J., G. Sarmiento, and R. E. Narrete. 2000. "The Stratigraphy of the W Side of the Cretaceous Colombian Basin in the Upper Magdalena Valley. Reevaluation of Selected Areas and Type Localities Including Aipe, Guaduas, Ortega, and Piedras." *Geología Colombiana* 25: 45–110.

Gutiérrez, E. G., B. K. Horton, C. Vallejo, L. J. Jackson, and S. W. George. 2019. "Provenance and Geochronological Insights into Late Cretaceous-Cenozoic Foreland Basin Development in the Subandean

13652117, 2025, 3, Downloaded from https://onlinelibrary.wiley.com/doi/10.1111/bre.70041 by Cochrane Colombia, Wiley Online Library on [20/06/2025]. See the Terms and Conditions (https://onlinelibrary.wiley.com/terms-and-conditions) on Wiley Online Library for rules of use; OA articles are governed by the applicable Creative Commons License

Zone and Oriente Basin of Ecuador." In *Andean Tectonics*, 237–268. Elsevier.

Higley, D. K. 2001. "The Putumayo-Oriente-Maranon Province of Colombia, Ecuador, and Peru." *Mesozoic-Cenozoic and Paleozoic Petroleum Systems* (No. 63).

Hoorn, C., F. P. Wesselingh, H. Ter Steege, et al. 2010. "Amazonia Through Time: Andean Uplift, Climate Change, Landscape Evolution, and Biodiversity." *Science* 330, no. 6006: 927–931.

Horton, B. K. 2018. "Sedimentary Record of Andean Mountain Building." *Earth-Science Reviews* 178: 279–309.

Horton, B. K., T. N. Capaldi, C. Mackaman-Lofland, et al. 2022. "Broken Foreland Basins and the Influence of Subduction Dynamics, Tectonic Inheritance, and Mechanical Triggers." *Earth-Science Reviews* 234: 104193.

Horton, B. K., F. Fuentes, A. Boll, D. Starck, S. G. Ramirez, and D. F. Stockli. 2016. "Andean Stratigraphic Record of the Transition From Backarc Extension to Orogenic Shortening: A Case Study From the Northern Neuquén Basin, Argentina." *Journal of South American Earth Sciences* 71: 17–40.

Horton, B. K., M. Parra, and A. Mora. 2020. "Construction of the Eastern Cordillera of Colombia: Insights From the Sedimentary Record." In *The Geology of Colombia, Volume 3 Paleogene – Neogene*, edited by J. Gómez and D. Mateus-Zabala, 22 p. Bogotá. Servicio Geológico Colombiano, Publicaciones Geológicas Especiales 37. https://doi.org/10.32685/pub.esp.37.2019.03.

Horton, B. K., J. E. Saylor, J. Nie, et al. 2010. "Linking Sedimentation in the Northern Andes to Basement Configuration, Mesozoic Extension, and Cenozoic Shortening: Evidence From Detrital Zircon U-Pb Ages, Eastern Cordillera, Colombia." *Geological Society of America Bulletin* 122, no. 9–10: 1423–1442.

Hurtado, C., M. Roddaz, R. V. Santos, P. Baby, P. O. Antoine, and E. L. Dantas. 2018. "Cretaceous-Early Paleocene Drainage Shift of Amazonian Rivers Driven by Equatorial Atlantic Ocean Opening and Andean Uplift as Deduced From the Provenance of Northern Peruvian Sedimentary Rocks (Huallaga Basin)." *Gondwana Research* 63: 152–168.

Ibañez-Mejia, M. 2020. "The Putumayo Orogen of Amazonia: A Synthesis." In *The Geology of Colombia, Volume 1 Proterozoic – Paleozoic*, edited by J. Gómez and D. Mateus-Zabala, 101–131. Bogotá. Neogene. Servicio Geológico Colombiano, Publicaciones Geológicas Especiales 35. https://doi.org/10.32685/pub.esp.35.2019.06.

Ibanez-Mejia, M., E. M. Bloch, and J. D. Vervoort. 2018. "Timescales of Collisional Metamorphism From Sm-Nd, Lu-Hf and U-Pb Thermochronology: A Case From the Proterozoic Putumayo Orogen of Amazonia." *Geochimica et Cosmochimica Acta* 235: 103–126.

Ibanez-Mejia, M., A. Pullen, J. Arenstein, et al. 2015. "Unraveling Crustal Growth and Reworking Processes in Complex Zircons From Orogenic Lower-Crust: The Proterozoic Putumayo Orogen of Amazonia." *Precambrian Research* 267: 285–310.

Ibanez-Mejia, M., J. Ruiz, V. A. Valencia, A. Cardona, G. E. Gehrels, and A. R. Mora. 2011. "The Putumayo Orogen of Amazonia and Its Implications for Rodinia Reconstructions: New U-Pb Geochronological Insights Into the Proterozoic Tectonic Evolution of Northwestern South America." *Precambrian Research* 191, no. 1–2: 58–77.

Idárraga García, J., J. M. Kendall, and C. A. Vargas. 2016. "Shear Wave Anisotropy in Northwestern South America and Its Link to the Caribbean and Nazca Subduction Geodynamics." *Geochemistry, Geophysics, Geosystems* 17, no. 9: 3655–3673.

Ingersoll, R. V., T. F. Bullard, R. L. Ford, J. P. Grimm, J. D. Pickle, and S. W. Sares. 1984. "The Effect of Grain Size on Detrital Modes: A Test of the Gazzi-Dickinson Point- Counting Method." *Journal of Sedimentary Petrology* 54, no. 1: 103–116.

Jaillard, E., H. Lapierre, M. Ordonez, J. T. Alava, A. Amortegui, and J. Vanmelle. 2009. "Accreted Oceanic Terranes in Ecuador: Southern Edge of the Caribbean Plate?" *Geological Society, London, Special Publications* 328, no. 1: 469–485.

Jaramillo, J. S., A. Cardona, S. León, V. Valencia, and C. Vinasco. 2017. "Geochemistry and Geochronology From Cretaceous Magmatic and Sedimentary Rocks at 6 35′ N, Western Flank of the Central Cordillera (Colombian Andes): Magmatic Record of Arc Growth and Collision." *Journal of South American Earth Sciences* 76: 460–481.

Jaramillo, J. S., S. Zapata, M. Carvalho, et al. 2022. "Diverse Magmatic Evolutionary Trends of the Northern Andes Unraveled by Paleocene to Early Eocene Detrital Zircon Geochemistry." *Geochemistry, Geophysics, Geosystems* 23, no. 9: e2021GC010113.

Jones, M. A., P. L. Heller, E. Roca, M. Garcés, and L. Cabrera. 2004. "Time Lag of Syntectonic Sedimentation Across an Alluvial Basin: Theory and Example From the Ebro Basin, Spain." *Basin Research* 16, no. 4: 489–506.

Kern, A. K., M. Gross, C. P. Galeazzi, et al. 2020. "Re-Investigating Miocene Age Control and Paleoenvironmental Reconstructions in Western Amazonia (Northwestern Solimões Basin, Brazil)." *Palaeogeography, Palaeoclimatology, Palaeoecology* 545: 109652.

Kerr, A. C., J. Tarney, A. Nivia, G. Marriner, and A. Saunders. 1996. "The Geochemistry and Tectonic Setting of Late Cretaceous Caribbean and Colombian Volcanism." *Journal of South American Earth Sciences* 9: 1–2.

Laul, J. C. 1979. "Neutron Activation Analysis of Geological Materials." *Atomic Energy Review* 17, no. 3: 603–695.

Lawton, T. F. 2019. "Laramide Sedimentary Basins and Sediment-Dispersal Systems." In *The Sedimentary Basins of the United States and Canada*, 529–557. Elsevier.

Lawton, T. F., P. Homewood, and P. A. Allen. 1986. "Compositional Trends Within a Clastic Wedge Adjacent to a Fold-Thrust Belt: Indianola Group, Central Utah, USA." *Foreland Basins* 8: 411–423.

Leal-Mejía, H., R. P. Shaw, and J. C. Melgarejo i Draper. 2019. "Spatial-Temporal Migration of Granitoid Magmatism and the Phanerozoic Tectono-Magmatic Evolution of the Colombian Andes." In *Geology and Tectonics of Northwestern South America. Frontiers in Earth Sciences*, edited by F. Cediel and R. P. Shaw, 253–410. Springer. https://doi.org/10.1007/978-3-319-76132-9_5.

León, S., S. Jiménez-Rodríguez, A. Piraquive, et al. 2023. "Sediment Provenance Signal of the Discontinuous Retroarc Topography in the Northern Andes During the Early Cretaceous." *Terra Nova* 35, no. 5: 440–449.

León, S., A. Cardona, M. Parra, et al. 2018. "Transition From Collisional to Subduction-Related Regimes: An Example From Neogene Panama-Nazca-South America Interactions." *Tectonics* 37, no. 1: 119–139.

León, S., G. Monsalve, and C. Bustamante. 2021. "How Much Did the Colombian Andes Rise by the Collision of the Caribbean Oceanic Plateau?" *Geophysical Research Letters* 48, no. 7: e2021GL093362.

Liu, X., and C. A. Currie. 2019. "Influence of Upper Plate Structure on Flat-Slab Depth: Numerical Modeling of Subduction Dynamics." *Journal of Geophysical Research: Solid Earth* 124, no. 12: 13150–13167.

Liu, L., M. Gurnis, M. Seton, J. Saleeby, R. D. Müller, and J. M. Jackson. 2010. "The Role of Oceanic Plateau Subduction in the Laramide Orogeny." *Nature Geoscience* 3, no. 5: 353–357.

Londoño, J. 2004. *Foreland Basins: Lithospheric Flexure, Plate Strength and Regional Stratigraphy*. Louisiana State University and Agricultural & Mechanical College.

Londoño, J., J. M. Lorenzo, and V. Ramirez. 2012. *Lithospheric Flexure and Related Base-Level Stratigraphic Cycles in Continental Foreland Basins: An Example From the Putumayo Basin, Northern Andes*.

13652117, 2025, 3, Downloaded from https://onlinelibrary.wiley.com/doi/10.1111/bre.70041 by Cochrane Colombia, Wiley Online Library on [20/06/2025]. See the Terms and Conditions (https://onlinelibrary.wiley.com/terms-and-conditions) on Wiley Online Library for rules of use; OA articles are governed by the applicable Creative Commons License

Louterbach, M., M. Roddaz, P. O. Antoine, et al. 2018. "Provenance Record of Late Maastrichtian–Late Palaeocene Andean Mountain Building in the Amazonian Retroarc Foreland Basin (Madre de Dios Basin, Peru)." *Terra Nova* 30, no. 1: 17–23.

Louterbach, M., M. Roddaz, J. Bailleul, et al. 2014. "Evidences for a Paleocene Marine Incursion in Southern Amazonia (Madre de Dios Sub-Andean Zone, Peru)." *Palaeogeography, Palaeoclimatology, Palaeoecology* 414: 451–471.

Martinez, M. 2010. "Petrogénesis de las vulcanitas estratificadas en sedimentitas del Cretácico Superior, Río Guaguaquí, flanco occidental de la Cordillera Oriental." Undergraduate thesis, Universidad Nacional de Colombia.

Martin-Gombojav, N., and W. Winkler. 2008. "Recycling of Proterozoic Crust in the Andean Amazon Foreland of Ecuador: Implications for Orogenic Development of the Northern Andes." *Terra Nova* 20, no. 1: 22–31.

Maya, M., and H. González. 1995. "Unidades Litodémicas en la Cordillera Central de Colombia." *Boletín Geológico* 35, no. 2–3: 44–57.

McCourt, W. J., J. A. Aspden, and M. Brook. 1984. "New Geological and Geochronological Data From the Colombian Andes: Continental Growth by Multiple Accretion." *Journal of the Geological Society* 141: 14p–845p.

Miall, A. D. 1985. "Architectural-Element Analysis: A New Method of Facies Analysis Applied to Fluvial Deposits." *Earth-Science Reviews* 22, no. 4: 261–308.

Miall, A. D. 2006. "Lithofacies." In *The Geology of Fluvial Deposits*, 99–130. Springer.

Mojica, J. 1980. "Observaciones Acerca del Estado Actual del Conocimiento de la Formación Payandé (Triásico Superior), Valle Superior del Río Magdalena, Colombia." *Geología Colombiana* 11: 67–88.

Mojica, J., and P. Prinz-Grimm. 2000. "La Fauna de Amonitas del Triásico Tardío en el Miembro Chicalá (Parte Baja de la Formación Saldaña) en Payandé, Tolima, Colombia." *Geología Colombiana* 25: 13–23.

Montes, C., A. Cardona, R. McFadden, et al. 2012. "Evidence for Middle Eocene and Younger Land Emergence in Central Panama: Implications for Isthmus Closure." *Geological Society of America Bulletin* 124, no. 5–6: 780–799.

Montes, C., and N. Hoyos. 2020. "Isthmian Bedrock Geology: Tilted, Bent, and Broken." In *The Geology of Colombia, Volume 3 Paleogene – Neogene. Servicio Geológico Colombiano, Publicaciones Geológicas Especiales*, edited by J. Gómez and D. Mateus–Zabala, 37, 451–467. https://doi.org/10.32685/pub.esp.37.2019.15.

Montes, C., A. F. Rodriguez-Corcho, G. Bayona, N. Hoyos, S. Zapata, and A. Cardona. 2019. "Continental Margin Response to Multiple Arc-Continent Collisions: The Northern Andes-Caribbean Margin." *Earth-Science Reviews* 198: 102903.

Montenegro, G., and M. Barragán. 2011. *Caguan and Putumayo Basins*. Vol. 4, 126. ANH-University EAFIT. Department of Geology.

Montes, C., C. A. Silva, G. A. Bayona, et al. 2021. "A Middle to Late Miocene Trans-Andean Portal: Geologic Record in the Tatacoa Desert." *Frontiers in Earth Science* 8. https://doi.org/10.3389/feart.2020.587022.

Mora, A., T. Gaona, J. Kley, et al. 2009. "The Role of Inherited Extensional Fault Segmentation and Linkage in Contractional Orogenesis: A Reconstruction of Lower Cretaceous Inverted Rift Basins in the Eastern Cordillera of Colombia." *Basin Research* 21, no. 1: 111–137.

Mora, A., M. Parra, M. R. Strecker, A. Kammer, C. Dimaté, and F. Rodríguez. 2006. "Cenozoic Contractional Reactivation of Mesozoic Extensional Structures in the Eastern Cordillera of Colombia." *Tectonics* 25, no. 2: 1–19.

Mora, A., D. Venegas, and L. Vergara. 1998. "Estratigrafía del Cretácico Superior y Terciario Inferior en el Sector Norte de la Cuenca del Putumayo, Departamento del Caquetá, Colombia." *Geología Colombiana* 23: 31–77.

Mora, A., A. Reyes-Harker, G. Rodriguez, et al. 2013. "Inversion Tectonics Under Increasing Rates of Shortening and Sedimentation: Cenozoic Example From the Eastern Cordillera of Colombia." *Geological Society, London, Special Publications* 377, no. 1: 411–442. https://doi.org/10.1144/sp377.6.

Mora, A., D. Villagómez, M. Parra, et al. 2020. "Late Cretaceous to Cenozoic Uplift of the Northern Andes: Paleogeographic Implications." In *The Geology of Colombia, Volume 3 Paleogene – Neogene*, edited by J. Gómez and D. Mateus–Zabala, 89–121. Servicio Geológico Colombiano, Publicaciones Geológicas Especiales 37. https://doi.org/10.32685/pub.esp.37.2019.04.

Moyano-Nieto, I. E., G. A. Prieto, and M. Ibañez-Mejia. 2022. "Tectonic Domains in the NW Amazonian Craton From Geophysical and Geological Data." *Precambrian Research* 377: 106735.

Mulch, A. 2016. "Stable Isotope Paleoaltimetry and the Evolution of Landscapes and Life." *Earth and Planetary Science Letters* 433: 180–191.

Najman, Y., A. Carter, G. Oliver, and E. Garzanti. 2005. "Provenance of Eocene Foreland Basin Sediments, Nepal: Constraints to the Timing and Diachroneity of Early Himalayan Orogenesis." *Geology* 33, no. 4: 309–312.

Nie, J., B. K. Horton, A. Mora, et al. 2010. "Tracking Exhumation of Andean Ranges Bounding the Middle Magdalena Valley Basin, Colombia." *Geology* 38, no. 5: 451–454.

Nie, J., B. K. Horton, J. E. Saylor, et al. 2012. "Integrated Provenance Analysis of a Convergent Retroarc Foreland System: U-Pb Ages, Heavy Minerals, Nd Isotopes, and Sandstone Compositions of the Middle Magdalena Valley Basin, Northern Andes, Colombia." *Earth-Science Reviews* 110, no. 1–4: 111–126.

Núñez, A. 2003. Reconocimiento geológico regional de las planchas 411 La Cruz, 412 San Juan de Villalobos, 430 Mocoa, 431 Piamonte, 448 Monopamba, 449 Fiorito y 465 Churuyaco. Memoria explicativa, escala, 1(100.000).

Odlum, M. L., D. F. Stockli, T. N. Capaldi, et al. 2019. "Tectonic and Sediment Provenance Evolution of the South Eastern Pyrenean Foreland Basins During Rift Margin Inversion and Orogenic Uplift." *Tectonophysics* 765: 226–248.

Osorio, C., D. Michoux, and G. Tellez. 2002. *Stratigraphy of the Tertiary Sequences-Upper Magdalena and the Putumayo Basins, a Different Point of View for Hydrocarbon Exploration*, 10. Memorias de la Segunda Convención técnica de la Asociación Colombiana de Geólogos y Geofísicos del Petróleo.

O'Sullivan, G., D. Chew, G. Kenny, I. Henrichs, and D. Mulligan. 2020. "The Trace Element Composition of Apatite and Its Application to Detrital Provenance Studies." *Earth-Science Reviews* 201: 103044.

O'Sullivan, G. J., D. M. Chew, A. C. Morton, C. Mark, and I. A. Henrichs. 2018. "An Integrated Apatite Geochronology and Geochemistry Tool for Sedimentary Provenance Analysis." *Geochemistry, Geophysics, Geosystems* 19, no. 4: 1309–1326.

Paces, J. B., and J. D. Miller Jr. 1993. "Precise U-Pb ages of Duluth Complex and Related Mafic Intrusions, Northeastern Minnesota: Geochronological Insights to Physical, Petrogenetic, Paleomagnetic, and Tectonomagmatic Processes Associated With the 1.1 Ga Midcontinent Rift System." *Journal of Geophysical Research: Solid Earth* 98, no. B8: 13997–14013.

Pachón-Parra, L. F., P. Mann, and N. Cardozo. 2020. "Regional Subsurface Mapping and 3D Flexural Modeling of the Obliquely Converging Putumayo Foreland Basin, Southern Colombia." *Interpretation* 8, no. 4: ST15–ST48.

13652117, 2025, 3, Downloaded from https://onlinelibrary.wiley.com/doi/10.1111/bre.70041 by Cochrane Colombia, Wiley Online Library on [20/06/2025]. See the Terms and Conditions (https://onlinelibrary.wiley.com/terms-and-conditions) on Wiley Online Library for rules of use; OA articles are governed by the applicable Creative Commons License

Parra, M., A. Mora, C. Jaramillo, et al. 2009. "Orogenic Wedge Advance in the Northern Andes: Evidence From the Oligocene-Miocene Sedimentary Record of the Medina Basin, Eastern Cordillera, Colombia." *Geological Society of America Bulletin* 121, no. 5–6: 780–800.

Parra, M., A. Mora, C. Lopez, L. Ernesto Rojas, and B. K. Horton. 2012. "Detecting Earliest Shortening and Deformation Advance in Thrust Belt Hinterlands: Example From the Colombian Andes." *Geology* 40, no. 2: 175–178.

Parra, M., A. Mora, C. Jaramillo, V. Torres, G. Zeilinger, and M. R. Strecker. 2010. "Tectonic Controls on Cenozoic Foreland Basin Development in the North-Eastern Andes, Colombia." *Basin Research* 22, no. 6: 874–903.

Paton, C., J. Hellstrom, B. Paul, J. Woodhead, and J. Hergt. 2011. "Iolite: Freeware for the Visualisation and Processing of Mass Spectrometric Data." *Journal of Analytical Atomic Spectrometry* 26, no. 12: 2508–2518.

Paul, A. N., R. A. Spikings, D. Chew, and J. S. Daly. 2019. "The Effect of Intra-Crystal Uranium Zonation on Apatite U-Pb Thermochronology: A Combined ID-TIMS and LA-MC-ICP-MS Study." *Geochimica et Cosmochimica Acta* 251: 15–35.

Pindell, J. L., and L. Kennan. 2009. "Tectonic Evolution of the Gulf of Mexico, Caribbean and Northern South America in the Mantle Reference Frame: An Update." *Geological Society, London, Special Publications* 328, no. 1: 1–55.

Priem, H. N. A., S. B. Kroonenberg, N. A. I. M. Boelrijk, and E. H. Hebeda. 1989. "Rb-Sr and K-Ar Evidence for the Presence of a 1.6 Ga Basement Underlying the 1.2 Ga Garzón-Santa Marta Granulite Belt in the Colombian Andes." *Precambrian Research* 42, no. 3–4: 315–324.

Ramos, V. A., and A. Folguera. 2005. "Tectonic Evolution of the Andes of Neuquén: Constraints Derived From the Magmatic Arc and Foreland Deformation." *Geological Society, London, Special Publications* 252, no. 1: 15–35.

Restrepo, M., C. Bustamante, A. Cardona, et al. 2021. "Tectonic Implications of the Jurassic Magmatism and the Metamorphic Record at the Southern Colombian Andes." *Journal of South American Earth Sciences* 111: 103439.

Riel, N., J. C. Duarte, J. Almeida, et al. 2023. "Subduction Initiation Triggered the Caribbean Large Igneous Province." *Nature Communications* 14, no. 1: 786.

Roddaz, M., W. Hermoza, A. Mora, et al. 2010. "Cenozoic Sedimentary Evolution of the Amazonian Foreland Basin System." In *Amazonia, Landscape and Species Evolution: a Look Into the Past*, vol. 5, 61–88. Blackwell-Wiley.

Rodríguez, G., M. I. Arango, G. Zapata, and J. G. Bermúdez. 2018. "Petrotectonic Characteristics, Geochemistry, and U-Pb Geochronology of Jurassic Plutons in the Upper Magdalena Valley-Colombia: Implications on the Evolution of Magmatic Arcs in the NW Andes." *Journal of South American Earth Sciences* 81: 10–30.

Rodríguez, G., G. Zapata, M. I. Arango, and J. G. Bermúdez. 2017. "Petrographic, Geochemistry and Geochronological Characterization of Permian Granitoids Rocks to the West of la Plata and Pacarní-Huila, Upper Magdalena Valley-Colombia." *Boletín de Geología* 39, no. 1: 41–68.

Roncancio, J., and M. Martínez. 2011. "Upper Magdalena Basin." In *Geology and Hydrocarbon Potential Regional Geology of Colombia Vol 14*. Agencia Nacional de Hidrocarburos. 182 p.

Ruiz, G. M. H. 2002. "Exhumation of the Northern Sub-Andean Zone of Ecuador and its Source Regions: A Combined Thermochronological and Heavy Mineral Approach." Doctoral dissertation, ETH Zurich.

Ruiz, G. M. H., D. Seward, and W. Winkler. 2004. "Detrital Thermochronology; a New Perspective on Hinterland Tectonics, an Example From the Andean Amazon Basin, Ecuador." *Basin Research* 16: 413–430.

Sacek, V. 2014. "Drainage Reversal of the Amazon River due to the Coupling of Surface and Lithospheric Processes." *Earth and Planetary Science Letters* 401: 301–312.

Saeid, E., K. B. Bakioglu, J. Kellogg, A. Leier, J. A. Martinez, and E. Guerrero. 2017. "Garzón Massif Basement Tectonics: Structural Control on Evolution of Petroleum Systems in Upper Magdalena and Putumayo Basins, Colombia." *Marine and Petroleum Geology* 88: 381–401.

Santos, C., C. Jaramillo, G. Bayona, M. Rueda, and V. Torres. 2008. "Late Eocene Marine Incursion in North-Western South America." *Palaeogeography, Palaeoclimatology, Palaeoecology* 264, no. 1–2: 140–146.

Sandoval, J. R., N. Pérez-Consuegra, A. Mora, et al. 2024. "Discrimination of Tectonic Provinces Using Zircon U-Pb Ages From Bedrock and Detrital Samples in the Northern Andes." *Geological Society of America Bulletin* 136, no. 11–12: 5231–5248.

Sarmiento-Rojas, L. F., J. D. Van Wess, and S. Cloetingh. 2006. "Mesozoic Transtensional Basin History of the Eastern Cordillera, Colombian Andes: Inferences From Tectonic Models." *Journal of South American Earth Sciences* 21, no. 4: 383–411.

Saylor, J. E., B. K. Horton, J. Nie, J. Corredor, and A. Mora. 2011. "Evaluating Foreland Basin Partitioning in the Northern Andes Using Cenozoic Fill of the Floresta Basin, Eastern Cordillera, Colombia." *Basin Research* 23: 377–402. https://doi.org/10.1111/j.1365-2117.2010.00493.x.

Schildgen, T. F., and P. A. van der Beek. 2019. "The Application of Low-Temperature Thermochronology to the Geomorphology of Orogenic Systems." In *Fission-Track Thermochronology and Its Application to Geology*, 335–350. Springer.

Schoene, B., and S. A. Bowring. 2006. "U-Pb Systematics of the McClure Mountain Syenite: Thermochronological Constraints on the Age of the 40Ar/39Ar Standard MMhb." *Contributions to Mineralogy and Petrology* 151, no. 5: 615–630.

SGC-ANH. 2022. "Unificación información geológica de superficie en un sistema integral basado en la cartografía para la subcuenca Caguán." 459p.

Siravo, G., C. Faccenna, M. Gérault, et al. 2019. "Slab Flattening and the Rise of the Eastern Cordillera, Colombia." *Earth and Planetary Science Letters* 512: 100–110.

Soares, C. J., S. Guedes, J. C. Hadler, R. Mertz-Kraus, and T. Zack. 2014. "Novel Calibration for LA-ICP-MS-Based Fission-Track Thermochronology." *Physics and Chemistry of Minerals* 41: 65–73. https://doi.org/10.1007/s00269-013-0624-2.

Somoza, R. 1998. "Updated Nazca (Farallon)—South America Relative Motions During the Last 40 My: Implications for Mountain Building in the Central Andean Region." *Journal of South American Earth Sciences* 11, no. 3: 211–215.

Spikings, R. A., P. V. Crowhurst, W. Winkler, and D. Villagomez. 2010. "Syn-and Post-Accretionary Cooling History of the Ecuadorian Andes Constrained by Their In-Situ and Detrital Thermochronometric Record." *Journal of South American Earth Sciences* 30, no. 3–4: 121–133.

Spikings, R. A., D. Seward, W. Winkler, and G. M. Ruiz. 2000. "Low-Temperature Thermochronology of the Northern Cordillera Real, Ecuador: Tectonic Insights From Zircon and Apatite Fission Track Analysis." *Tectonics* 19, no. 4: 649–668.

Spikings, R., and G. Simpson. 2014. "Rock Uplift and Exhumation of Continental Margins by the Collision, Accretion, and Subduction of Buoyant and Topographically Prominent Oceanic Crust." *Tectonics* 33, no. 5: 635–655.

13652117, 2025, 3, Downloaded from https://onlinelibrary.wiley.com/doi/10.1111/bre.70041 by Cochrane Colombia, Wiley Online Library on [20/06/2025]. See the Terms and Conditions (https://onlinelibrary.wiley.com/terms-and-conditions) on Wiley Online Library for rules of use; OA articles are governed by the applicable Creative Commons License

Spikings, R. A., W. Winkler, D. Seward, and R. Handler. 2001. "Along-Strike Variations in the Thermal and Tectonic Response of the Continental Ecuadorian Andes to the Collision With Heterogeneous Oceanic Crust." *Earth and Planetary Science Letters* 186, no. 1: 57–73.

Spotila, J. A. 2005. "Applications of Low-Temperature Thermochronometry to Quantification of Recent Exhumation in Mountain Belts." *Reviews in Mineralogy and Geochemistry* 58, no. 1: 449–466.

Strecker, M. R., G. E. Hilley, B. Bookhagen, and E. R. Sobel. 2011. "Structural, Geomorphic, and Depositional Characteristics of Contiguous and Broken Foreland Basins: Examples From the Eastern Flanks of the Central Andes in Bolivia and NW Argentina." In *Tectonics of Sedimentary Basins: Recent Advances*, 508–521. Blackwell.

Sylvester, P. J., A. K. Souders, and R. Liu. 2022. "Significance of U-Pb Detrital Zircon Geochronology for Mudstone Provenance." *Geology* 50, no. 6: 670–675.

Tassinari, C. C., and M. J. Macambira. 1999. "Geochronological Provinces of the Amazonian Craton." *Episodes* 22, no. 3: 174–182.

Thomson, S. N., G. E. Gehrels, J. Ruiz, and R. Buchwaldt. 2012. "Routine Low-Damage Apatite U-Pb Dating Using Laser Ablation–Multicollector–ICPMS." *Geochemistry, Geophysics, Geosystems* 13, no. 2: 1–23.

Valencia-Gómez, J. C., A. Cardona, G. Bayona, V. Valencia, and S. Zapata. 2020. "Análisis de Procedencia del Registro Sin-Orogénico Maastrichtiano de la Formación Cimarrona, Flanco Occidental de la Cordillera Oriental Colombiana." *Boletín de Geología* 42, no. 3: 171–204.

Vallejo, C., C. Romero, B. K. Horton, et al. 2021. "Jurassic to Early Paleogene Sedimentation in the Amazon Region of Ecuador: Implications for the Paleogeographic Evolution of Northwestern South America." *Global and Planetary Change* 204: 103555.

Vallejo, C., R. A. Spikings, L. Luzieux, W. Winkler, D. Chew, and L. Page. 2006. "The Early Interaction Between the Caribbean Plateau and the NW South American Plate." *Terra Nova* 18, no. 4: 264–269.

Vallejo, C., D. Tapia, J. Gaibor, et al. 2017. "Geology of the Campanian M1 Sandstone Oil Reservoir of Eastern Ecuador: A Delta System Sourced From the Amazon Craton." *Marine and Petroleum Geology* 86: 1207–1223.

van Der Wiel, A. M. 1991. *Uplift and Volcanism of the SE Colombian Andes in Relation to Neogene Sedimentation in the Upper Magdalena Valley*. Wageningen University and Research.

van Hinsbergen, D. J., and L. M. Boschman. 2019. "How High Were These Mountains?" *Science* 363, no. 6430: 928–929.

van Houten, F. B., and R. B. Travis. 1968. "Cenozoic Deposits, Upper Magdalena Valley, Colombia." *AAPG Bulletin* 52, no. 4: 675–702.

Vargas Gómez, Á. 2020. "Modelamiento del basamento y de la geometría de las cuencas presentes en la zona occidental de la región amazónica de Colombia y del norte del Ecuador, aplicando magnetometría y técnicas de inversión gravimétrica tridimensional." Master thesis, Universidad Nacional de Colombia. 97p.

Vallejo, C., W. Winkler, R. A. Spikings, L. Luzieux, F. Heller, and F. Bussy. 2009. "Mode and timing of terrane accretion in the forearc of the Andes in Ecuador." In *Backbone of the Americas: Shallow Subduction, Plateau Uplift, and Ridge and Terrane Collision*. Geological Society of America. https://doi.org/10.1130/2009.1204(09).

Vermeesch, P. 2018. "IsoplotR: A Free and Open Toolbox for Geochronology." *Geoscience Frontiers* 9: 1479–1493. https://doi.org/10.1016/j.gsf.2018.04.001.

Vermeesch, P. 2021. "Maximum Depositional Age Estimation Revisited." *Geoscience Frontiers* 12, no. 2: 843–850.

Villagomez, D. 2010. "Thermochronology, Geochronology and Geochemistry of the Western and Central Cordilleras and Sierra Nevada de Santa Marta, Colombia: The Tectonic Evolution of NW South America." Doctoral dissertation, University of Geneva.

Villagómez, D., and R. Spikings. 2013. "Thermochronology and Tectonics of the Central and Western Cordilleras of Colombia: Early Cretaceous–Tertiary Evolution of the Northern Andes." *Lithos* 160: 228–249.

Villagómez, D., R. Spikings, T. Magna, A. Kammer, W. Winkler, and A. Beltrán. 2011. "Geochronology, Geochemistry and Tectonic Evolution of the Western and Central Cordilleras of Colombia." *Lithos* 125, no. 3–4: 875–896.

Villamil, T., and C. Arango. 1998. "Integrated Stratigraphy of Latest Cenomanian and Early Turonian Facies of Colombia." In *Eustacy and Tectonostratigraphic Evolution of Northern South America*, edited by J. Pindell and C. Drake, 129–159. Society for Sedimentary Geology, Special Publication, Tulsa. https://doi.org/10.2110/pec.98.58.0129.

Villamizar-Escalante, N., M. Bernet, C. Urueña-Suárez, et al. 2021. "Thermal History of the Southern Central Cordillera and Its Exhumation Record in the Cenozoic Deposits of the Upper Magdalena Valley, Colombia." *Journal of South American Earth Sciences* 107: 103105.

Vinasco, C., and U. Cordani. 2012. "Reactivation Episodes of the Romeral Fault System in the Northwestern Part of Central Andes, Colombia, Through 39AR-40AR and K-Ar Results." *Boletín de Ciencias de la Tierra* 32: 111–124.

Weltje, G. J., and H. von Eynatten. 2004. "Quantitative Provenance Analysis of Sediments: Review and Outlook." *Sedimentary Geology* 171, no. 1–4: 1–11.

Wesselingh, F. P., J. Guerrero, M. E. Räsänen, L. Romero Pitmann, and H. B. Vonhof. 2006. "Landscape Evolution and Depositional Processes in the Miocene Pebas Lake/Wetland System: Evidence From Exploratory Boreholes in Northeastern Peru." *Scripta Geologica* 133: 323–361.

Wesselingh, F. P., M. E. Räsänen, G. Irion, et al. 2002. "Lake Pebas: A Palaeoecological Reconstruction of a Miocene, Long-Lived Lake Complex in Western Amazonia." *Cainozoic Research* 1: 35–81.

Wolaver, B. D., J. C. Coogan, B. K. Horton, et al. 2015. "Structural and Hydrogeologic Evolution of the Putumayo Basin and Adjacent Fold-Thrust Belt, Colombia." *AAPG Bulletin* 99, no. 10: 1893–1927.

Wolf, S. G., R. S. Huismans, J. A. Muñoz, M. E. Curry, and P. van der Beek. 2021. "Growth of Collisional Orogens From Small and Cold to Large and Hot—Inferences From Geodynamic Models." *Journal of Geophysical Research: Solid Earth* 126, no. 2: e2020JB021168. https://doi.org/10.1029/2020JB021168.

Yonkee, W. A., and A. B. Weil. 2015. "Tectonic Evolution of the Sevier and Laramide Belts Within the North American Cordillera Orogenic System." *Earth Science Reviews* 150: 531–593.

Zambrano, I., M. Ordoñez, and N. Jiménez. 1999. "Micropaleontologia de 63 muestras de afloramientos de la Cuenca Oriental Ecuatoriana." Informe tecnico No. 016-PPG-99, LABOGEO, Petroproducción, distrito de Guayaquil.

Zapata, S., L. Calderon-Diaz, C. Jaramillo, et al. 2023. "Drainage and Sedimentary Response of the Northern Andes and the Pebas System to Miocene Strike-Slip Tectonics: A Source to Sink Study of the Magdalena Basin." *Basin Research* 35, no. 5: 1674–1717.

Zapata, S., A. Cardona, J. S. Jaramillo, et al. 2019. "Cretaceous Extensional and Compressional Tectonics in the Northwestern Andes, Prior to the Collision With the Caribbean Oceanic Plateau." *Gondwana Research* 66: 207–226.

Zapata, S., A. Cardona, C. Jaramillo, V. Valencia, and J. Vervoort. 2016. "U-Pb LA-ICP-MS Geochronology and Geochemistry of Jurassic Volcanic and Plutonic Rocks From the Putumayo Region (Southern Colombia): Tectonic Setting and Regional Correlations." *Boletín de Geología* 38, no. 2: 21–38.

13652117, 2025, 3, Downloaded from https://onlinelibrary.wiley.com/doi/10.1111/bre.70041 by Cochrane Colombia, Wiley Online Library on [20/06/2025]. See the Terms and Conditions (https://onlinelibrary.wiley.com/terms-and-conditions) on Wiley Online Library for rules of use; OA articles are governed by the applicable Creative Commons License

Zapata-García, G., and G. Rodríguez-García. 2020. "New Contributions to the Knowledge of the Chocó–Panamá Arc in Colombia, Including a New Segment South of Colombia." In *The Geology of Colombia, Volume 3 Paleogene – Neogene*, edited by J. Gómez and D. Mateus-Zabala. Servicio Geológico Colombiano, Publicaciones Geológicas Especiales 37, 34 p. https://doi.org/10.32685/pub.esp.37.2019.14.

Supporting Information

Additional supporting information can be found online in the Supporting Information section.

13652117, 2025, 3, Downloaded from https://onlinelibrary.wiley.com/doi/10.1111/bre.70041 by Cochrane Colombia, Wiley Online Library on [20/06/2025]. See the Terms and Conditions (https://onlinelibrary.wiley.com/terms-and-conditions) on Wiley Online Library for rules of use; OA articles are governed by the applicable Creative Commons License